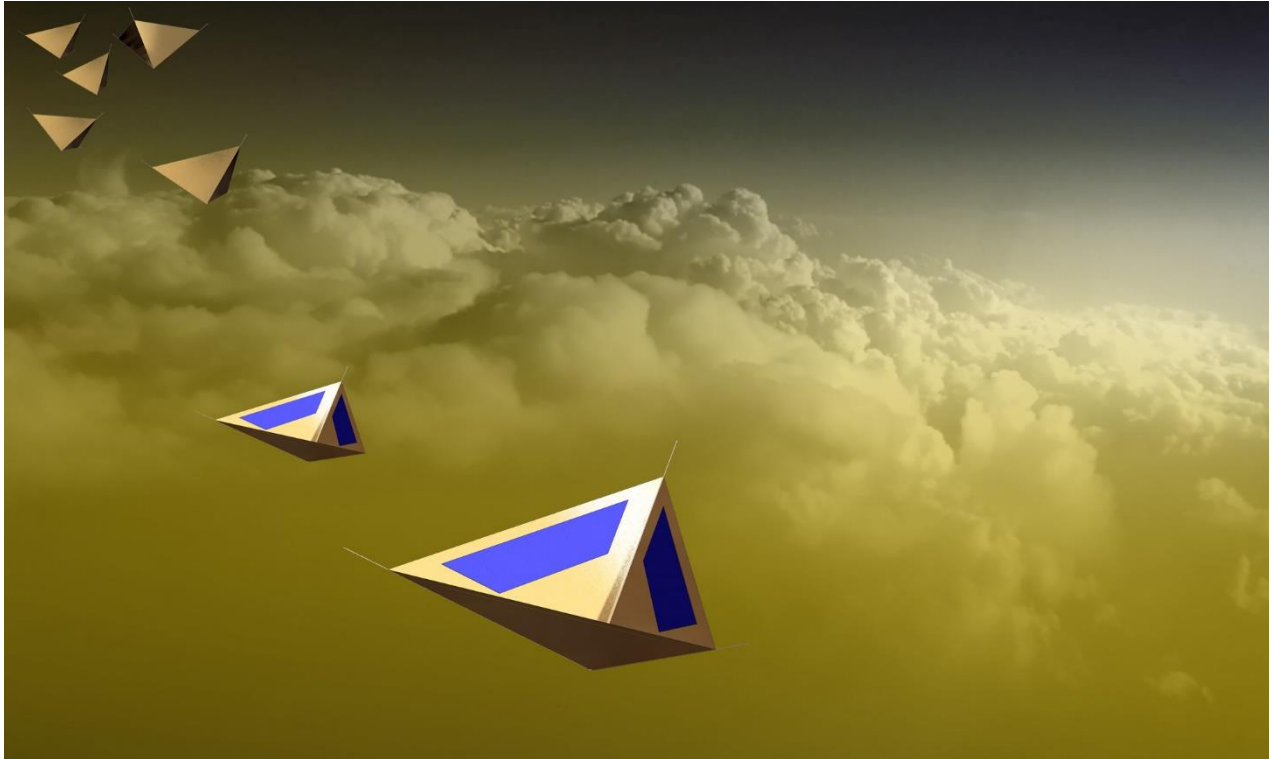


# LEAVES

Lofted Environmental and Atmospheric Venus Sensors



NASA Innovative Advanced Concepts

Phase I - Final Report

Solicitation: NNH17ZOA001N-18NIAC\_A1

Jeffrey Balcerski, P.I. - Ohio Aerospace Institute

*jeffreybalcerski@oai.org*

Gary Hunter – NASA Glenn Research Center

Darby Makel – Makel Engineering, Inc.

Anthony Colozza – Vantage Partners, LLC

Maciej Zborowski – Vantage Partners, LLC

# 1 TABLE OF CONTENTS

---

2	Summary.....	5
3	Science Motivation – The Closest Mystery.....	5
4	Design Requirements.....	7
4.1	Slow Descent.....	7
4.2	Geolocation.....	7
4.3	Chemical and Physical Environmental Data.....	8
5	Atmospheric Probe Design.....	8
5.1	Structure.....	8
5.2	Payload Overview.....	16
5.3	Sensors.....	17
5.4	Electronics.....	18
5.5	Tracking and Geolocation.....	19
5.6	Communications.....	23
5.7	Power.....	25
6	Swarming Venus – Design Reference Mission.....	27
6.1	Launch to Deployment.....	27
6.1.1	Entry Dynamics.....	27
6.2	Science Operations.....	29
7	Performance Trades and Options.....	31
7.1	Options for Mission Extension.....	31
7.1.1	Option 1 – Full science operation.....	31
7.1.2	Option 2 – Surface Survivability.....	32
8	Cost.....	33
9	Phase I Summary of Conclusions.....	33
10	References.....	35
11	Appendix.....	38
12	Acknowledgements.....	43

## Table of Figures

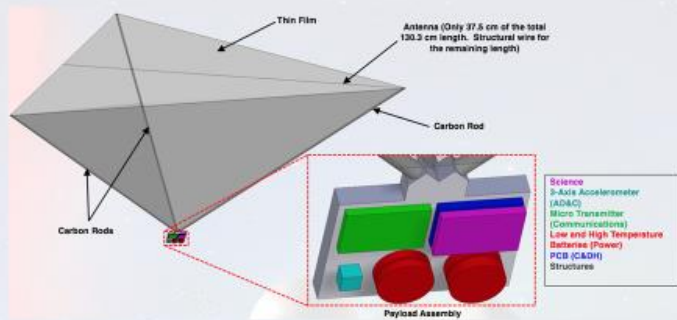
Figure 1. Venus' mysteries: Persistent gravity waves over high topography (left); Decadal cycles in upper atmosphere SO <sub>2</sub> (center); Increasing zonal wind velocity (right) .....	6
Figure 2. Model and profile of single LEAVES unit .....	9
Figure 3. Drag coefficients for wedges and cones. From Hoerner (1965).....	10
Figure 4. Reference atmospheric density at deployment altitude (shown in blue). From Mahieux et al. (2010).....	11
Figure 5. Peak load and heating from orbital entry simulation.....	11
Figure 6. Zonal wind speed versus altitude. From Peralta et al. (2017).....	12
Figure 7. Duration of science operations and time to surface contact after start of operations.....	13
Figure 8. Lateral drift distance versus time from start of science operations .....	13
Figure 9. Finite element model of maximum stress on panels.....	14
Figure 10. Finite element model of stress on carbon fiber struts .....	14
Figure 11. Sensitivity of deployment and descent conditions to areal density .....	15
Figure 12. LEAVES flat-packed stowing concept .....	16
Figure 13. Compact stowed configuration of 100 LEAVES units .....	16
Figure 14. Powered payload configuration.....	17
Figure 15. MEMS atmospheric sensor array. Credit - Makel Engineering, Inc. ....	17
Figure 16. Location of chemical sensors on payload.....	18
Figure 17. Command and data handling functional block diagram .....	19
Figure 18. Relative motion tracking assumptions.....	20
Figure 19. Demonstration of uncertainty in direct integration of position.....	20
Figure 20. (Left) Illustration of parallel reflection via triple orthogonal redirection. (Right) Array of corner retroreflectors at the Nevada Test Site. ....	21
Figure 21. Illustration of radar tracking study .....	22
Figure 22. Radar geometry analysis.....	22
Figure 23. Coincident probe locations along radar ray path.....	22
Figure 24. Radio link budget analysis.....	23
Figure 25. Radio radiation pattern analysis.....	24
Figure 26. Electrochem MR Series.....	26
Figure 27. Comparison of orbital decay times versus deployment altitude .....	28
Figure 28. Illustration of relationship of deployed LEAVES to orbiter during science operations.....	29
Figure 29. Orbiter radar footprint.....	30
Figure 30. Optimized orbital configuration for LEAVES radio contact and tracking .....	31
Figure 31. Prime contract cost estimate.....	33



# LEAVES Executive Summary



- LEAVES: Extremely light, Radar Retroreflectors with Sensors to probe Venus's atmosphere
- Conops: Probing the atmosphere at different times (dawn, noon, dusk, midnight) by 100 MEMS based ~120 g probes with combined radar reflector drag device can be performed using a Venus Radarsat during its aerobraking campaign (drop off orbit ~ 145 km x 10,000 km or lower), activated by atmospheric pressure after 'soft' entry
- Launch: Attached to side of future Venus Radarsat, 2020's opportunity
- Science: Chemical, pressure, temperature mems sensors and location data of ~1 Mb of data during 9 hour descent
- Mechanical: ~ 120 g "leaf" has 1 m<sup>2</sup> drag array that enables deployment in orbit and descent through atmosphere without aeroshell, ~ 12g loading at atmospheric deceleration over minutes of time
- Power: Two sets of batteries (low and high temp), ~ 250 mAh each at 3.5V
- C&DH: Microcontroller to store science data
- Comms: UHF transmitter, ~ 2 kbps to Radar Sat Relay
- AD&CS: Detect leaf movements with accelerometers for position matching with radar tracking back on earth
- Cost: \$50k to \$100K per leaf



Description	Basic Mass	Growth	Growth	Total Mass
	(kg)	(%)	(kg)	(kg)
Case 1 LEAVES CD-2010-155				
<b>LEAVES</b>	<b>0.1238</b>	<b>22.1%</b>	<b>0.0273</b>	<b>0.1511</b>
Leaf	0.1238	22.1%	0.0273	0.1511
Science	0.0056	30.4%	0.0017	0.0073
Attitude Determination and Control	0.0012	10.0%	0.0001	0.0013
Command & Data Handling	0.0130	30.4%	0.0039	0.169
Communications and Tracking	0.0155	10.0%	0.0016	0.171
Electrical Power Subsystem	0.0173	41.9%	0.0073	0.246
Structures and Mechanisms	0.0711	18.0%	0.0128	0.0840

## 2 SUMMARY

---

LEAVES (Lofted Environmental Atmospheric Venus Sensors) is a design exercise with the goal of dramatically decreasing the cost of obtaining prioritized chemical and physical data in planetary atmospheres. Through the application of a swarm approach this concept parallelizes atmospheric exploration, with geographic coverage far exceeding what is possible with conventional monolithic platforms or sondes. Each unit in the swarm is exceptionally compact, with a powered payload mass of only a few tens of grams and a high-drag, semi-rigid structure that acts to slow each probe as it descends through the atmosphere. This structural design can collapse into a planar form to allow for efficient stowage prior to arrival at the target body. With a total per-unit mass of only 120 g, a fleet of 100 (or more) units can be very reasonably accommodated on a carrier spacecraft.

Science operations, which begin when the LEAVES probes reach an altitude of 100 km, are targeted for the cloud-bearing region of Venus' atmosphere. During the roughly 9 hour, terminal velocity descent through the atmosphere, LEAVES collects data of the state and composition of the atmosphere in parallel across multiple units. These data would represent an unprecedented constraint on the distribution and concentration of targeted chemical species, and the detection of local and regional variations in both chemistry and physical properties.

A novel and compelling result of this exercise was that the same optimization that produced a structure with an exceptionally low areal mass density ( $0.126 \text{ kg/m}^2$ ) also resulted in a probe that can be deployed directly from an aerobraking orbit ( $\sim 140 \text{ km}$  at  $5 \text{ km/s}$ ) without the need for aeroshell protection. This translates to a tremendous mass savings and gives LEAVES the flexibility to be carried as a secondary payload aboard either a descending surface probe or an orbital radar mapper. Because such missions are under active development or have already been proposed (but not flown), we infer that LEAVES is well positioned as a technology demonstration or value-added component for near-term Venus flight opportunities.

## 3 SCIENCE MOTIVATION – THE CLOSEST MYSTERY

---

Venus, though the target of a veritable fleet of interplanetary probes in the 1970's and 1980's and easily accessible by planetary exploration standards, remains a profound mystery. From its slow retrograde rotation, to its lack of an intrinsic magnetic field, to its supercharged, arid, runaway greenhouse, Venus stands in extreme contrast to the lush and life-supporting environment of the Earth. That the two planets are so similar in mass and distance from the Sun (and presumably, initial composition) deepens the mystery and increases the need to understand what processes caused the two planets to evolve along completely different paths.

Because Venus' atmosphere is so dense, its internal dynamics and interactions with the surface are significant. This means that chemical changes in the atmosphere (i.e. from volcanic venting) can substantially affect the surface material; and changes in the surface (i.e. from faulting, impacts, or lava production) can substantially affect atmospheric chemistry. Thus, it is imperative to constrain, with high fidelity, the exact chemical compositions of both the surface and atmosphere. While surface mineralogical analysis often requires relatively massive equipment for sample retrieval, preparation, and assay, atmospheric gas analysis can be accomplished without the retrieval and preparation steps. In combination with the recent availability of high-precision, lightweight chemical sensors, this means that ultracompact aerial platforms are capable of obtaining valuable and high-priority science data.

A recent generation of Venus orbiters have highlighted the need for new *in situ* atmospheric data. For example, SO<sub>2</sub> concentrations at the cloud tops (synthesized from Magellan and Venus Express observations) show decadal cycles of pulses of higher concentrations of nearly an order of magnitude (Marcq, Bertaux, Montmessin, & Belyaev, 2013). SO<sub>2</sub>, being a major product of volcanic outgassing on the Earth, has no confirmed source or sink on Venus that could result in these dramatic changes. This indicates that either reactive species are being mobilized from the surface to the upper atmosphere (Esposito, 1984) or that there is some as-yet unknown process in the atmosphere that causes non-homogenous concentrations to be localized in time or geographic position (Zolotov, pers. communication, 2018). The Japanese Akatsuki mission has confirmed regional-scale standing waves coinciding with large surface topographic features and related to time of the solar day (Fukuhara et al., 2017). This means that near-surface winds are being redirected by surface topography to create vertical atmospheric structures that extend into the cloud tops. To add even more mystery, the velocity of upper zonal winds has been increasing over the last decade (Khatuntsev et al., 2013).

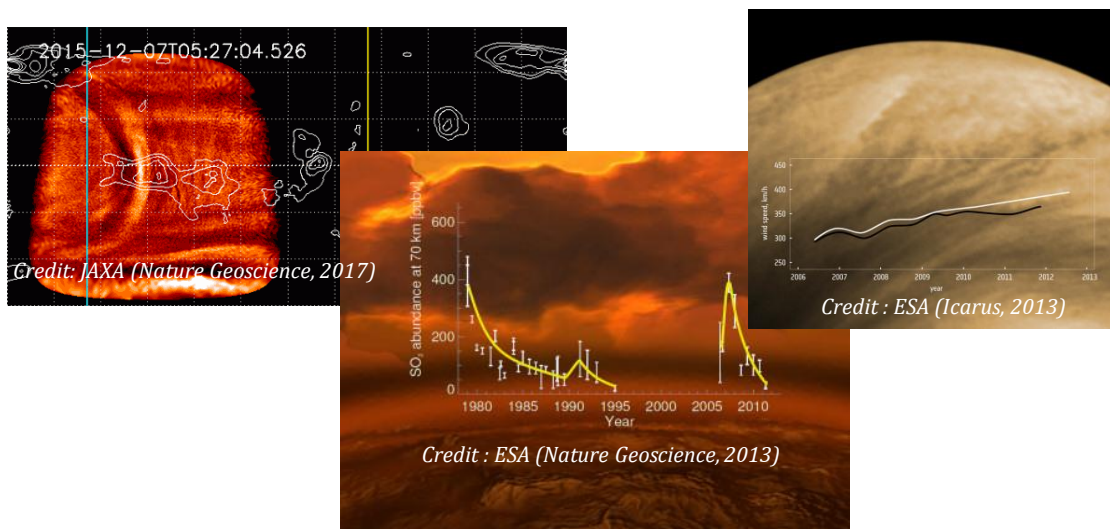


Figure 1. Venus' mysteries: Persistent gravity waves over high topography (left); Decadal cycles in upper atmosphere SO<sub>2</sub> (center); Increasing zonal wind velocity (right)

These relatively recent discoveries of the Venus atmosphere are in addition to other longstanding questions that remain unresolved, such as the nature of a UV-absorbing component of the atmosphere that accounts for 50% of absorbed solar radiation (Pollack et al., 1979; Yamazaki et al., 2018), or the mechanism responsible for continuous loss of carbonyl sulfide (Yung et al., 2009).

The use of ultralight swarms of sensors to investigate planetary environments has significant heritage in hypothetical studies, though none have flight heritage beyond low Earth orbit thus far (Bluman, Kang, Landrum, Fahimi, & Mesmer, n.d.; Cutts, Nock, Jones, Rodriguez, & Balaram, 1995; Petersen et al., 2017; Short, 2014; Young, 2001). Rather than attempt to reproduce these exercises for the surface of Venus, we chose to leverage the thick atmosphere for our benefit by focusing on lofted sensors platforms that are unguided and suspended only by the atmospheric drag over the descending structure. Thus, our study becomes an exercise of extreme minimization and seeks to answer the question, "What is the most science return that can be achieved for the least mass and cost?"

## **4 DESIGN REQUIREMENTS**

---

### **4.1 SLOW DESCENT**

A primary design consideration is maximizing the duration of science operations in the target altitudes of 100 to 30 km. This easily brackets the top and bottom layers of the clouds and at the lowest altitudes, a temperature of just over 200° C (Kliore, Keating, & Moroz, 1992). A traditional approach to slowing descent would be either a parachute/ballute or a positively buoyant balloon. Both of these options incur a mass penalty... the former with a canopy and rigging, and the latter with a membrane, rigging, and inflation media. Therefore, we addressed the question of the slowest possible descent by attempting to minimize mass while maximizing drag of an integrated structural body. The success criteria for this exercise was to significantly exceed the descent times of Venera, Vega, and Pioneer Venus probes and those currently in development or proposed. That is, we expected to significantly exceed a 1 hour descent time. At the other extreme is the ~46 hour flight time of the Vega balloons (J. E. Blamont et al., 1986) which we did not anticipate exceeding.

### **4.2 GEOLOCATION**

In order to maximize the value of continuous sampling of the atmosphere, we require that position (altitude, latitude, longitude) are able to be determined for a given timestamp for each LEAVES unit. The cloud-bearing atmosphere of Venus means that stars, surface features, and radio reference positioning (i.e. GPS) are all unavailable. Due to the low mass and power requirements, the approach used for the Vega balloons (J. Blamont, 1985), Very Long Baseline Interferometry (VLBI) is not a practical option. That is, LEAVES cannot support a radio transmitter capable of direct-to-Earth communication. We expected that some combination of active tracking, relative

positioning, pressure-based altimetry, and beacon-based navigation could provide this reference. We set our target spatial resolution to 10 km<sup>2</sup>, which is to say that a given measurement by a LEAVES unit could be resolved to a 10 x 10 km grid.

### **4.3 CHEMICAL AND PHYSICAL ENVIRONMENTAL DATA**

The driving science motivation for this exploration approach is the relative lack of data on the physical state (local and regional circulation and turbulence; temperature and pressure) and concentration of reactive chemical species throughout the atmospheric column and across a broad range of geographic locations. Prior atmospheric probes generally utilized gas chromatograph mass spectrometers, which are excellent for detection and characterization of unknown chemical species but in these cases had uncertainties that could exceed 20% concentration (Gel'man et al., 1979; Oyama et al., 1980). Therefore, a better than 5% uncertainty would represent at least a respectable improvement over existing data. For two of the primary active species (SO<sub>2</sub> and CO), that means an instrument sensitivity of around 1 ppm or better. Like the geolocation requirement above, we require that LEAVES samples the atmosphere with a high enough frequency such that the distance between measurements does not exceed 10 km. For temperature, we require a sensitivity of better than 1° C, which represents a nominal adiabatic change of 0.125 km, and a pressure sensitivity of better than 720 Pa, which is sufficient to resolve approximately 1 km of altitude change below 100 km (Kliore et al., 1992).

## **5 ATMOSPHERIC PROBE DESIGN**

---

### **5.1 STRUCTURE**

Our iterative structural design process was driven primarily by the slow-descent and geolocation requirements of Sections 4.1-4.2. Our preliminary design was a near-planar, square kite with a slightly low center of body / center of mass instrument payload. Although constructing a low-mass, high-drag structure has many possible options and solutions, the need to actively track the LEAVES units by an orbiting radar drove the shape choice. This portion of the study, and the choice of a cube-corner radar retroreflector is discussed in Section 5.4. Figure 2 below shows our choice of a 3-sided, inverted pyramid structure.



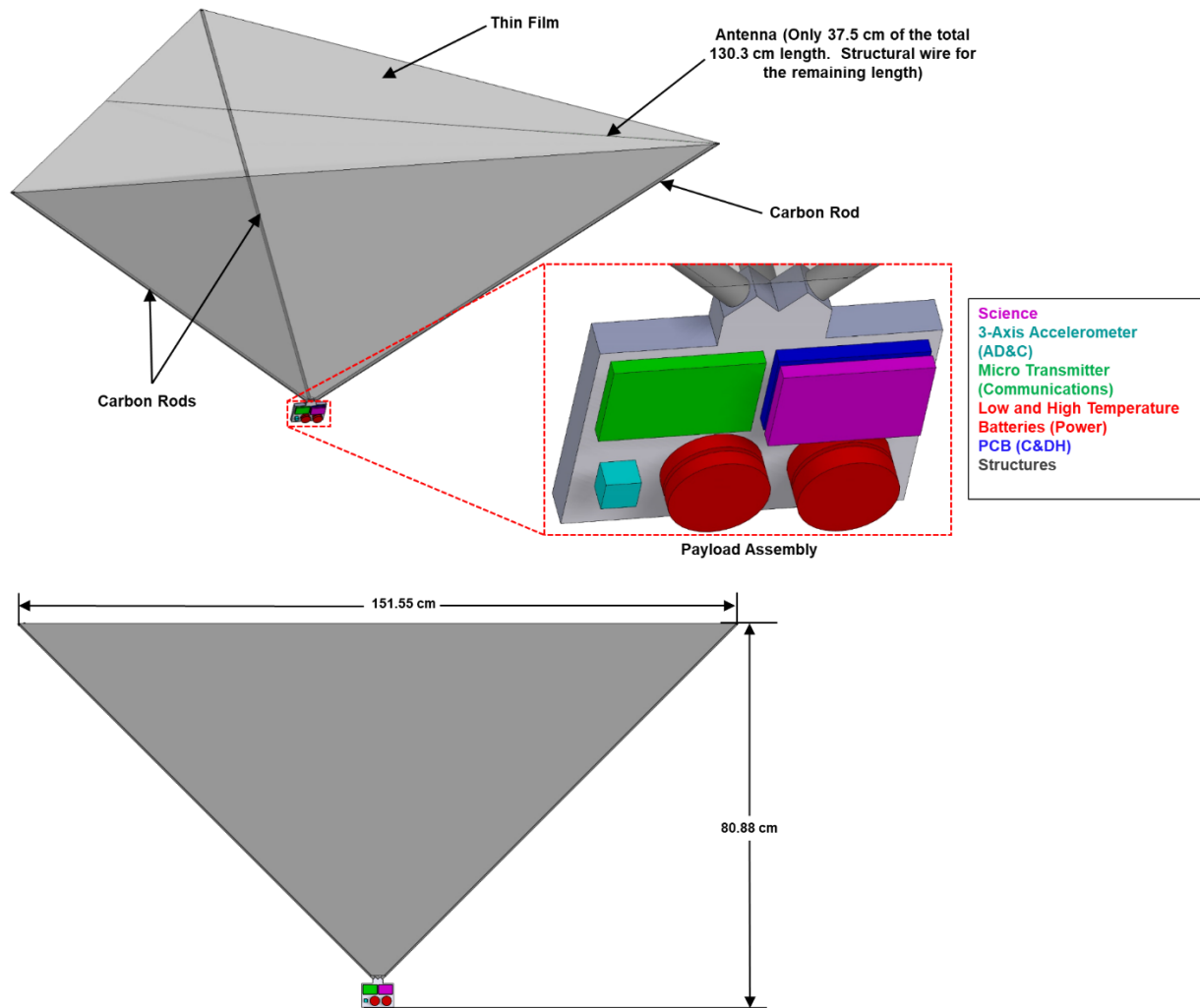
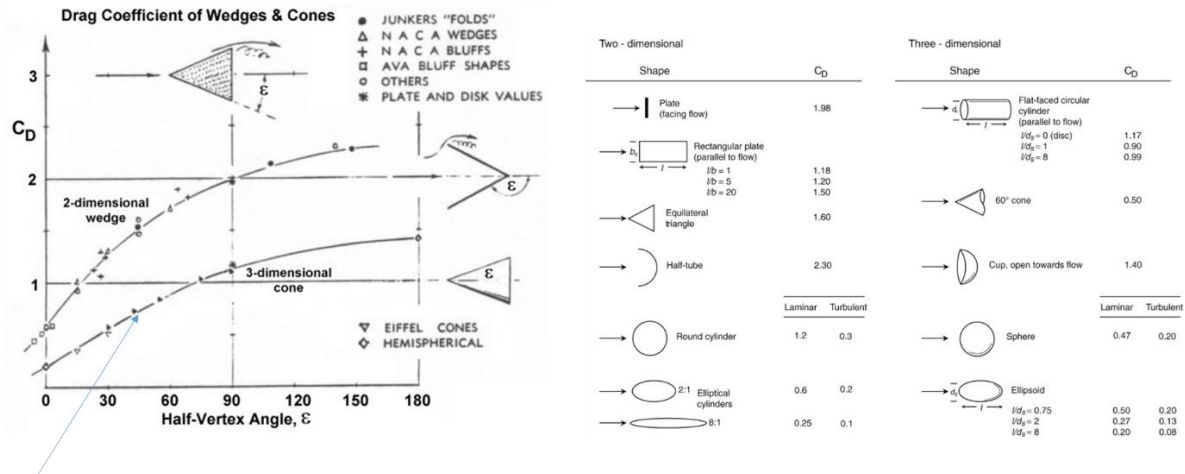


Figure 2. Model and profile of single LEAVES unit

Each of the three panels is a metalized, polyimide film (e.g. Kapton® by DuPont™). This is the least dense and most appropriate option, when compared to other possibilities such as Aluminum 6061-T6, polybenzoxazole (PBO), or polyimidobenzoxazole (PIBO) (Yavrouian, Plett, Yen, Cutts, & Baek, 1999). Each flexible panel is supported by 2 mm carbon fiber rods, commercially available for R/C aircraft and shown to be highly resistant to the thermal and chemical conditions of the Venus environment (private communication, J. Balcerski).

The dimensions shown above are the result of concurrent engineering exercises where structural area and mass was iterated with mass and power of the payload, deployment requirements, and lofted lifetime. In order to calculate the descent profile, along with the maximum force and heating that each unit will experience, we first estimated the drag coefficient ( $C_D$ ) of the three sided pyramid to be roughly that of a 3-dimensional cone. The  $C_D$  of a cone with a half-vertex angle of  $45^\circ$  (Figure 3) is taken from the figure in the canonical reference by Hoerner as 0.75 (Hoerner, 1965). We estimated atmospheric density by using a spectral fit to  $\text{CO}_2$  of the upper atmosphere

of the planet by the Venus Express mission (Mahieux et al., 2010) as shown in Figure 4. To test for maximum drag load and heating, we began a simulation at 300 km altitude, with an orbital entry angle of 5°, LEAVES mass of 130 g, aerodynamic profile (projected area) of 1 m<sup>2</sup> and entry velocity of 5.1 km/s. In these simulations, ballistic coefficient ( $\beta$ ) is given as:  $\beta = \frac{m}{C_D A}$  where  $m$  is mass,  $C_D$  is drag coefficient, and  $A$  is projected area. In this simulation and others that utilized a higher mass and deployment velocity, both peak heating and force occur between 109 and 112 km altitude. The results of this simulation can be seen in Figure 5.



For a 45° Half angle the 3-dimensional cone drag is estimated to be 0.75

Figure 3. Drag coefficients for wedges and cones. From Hoerner (1965).

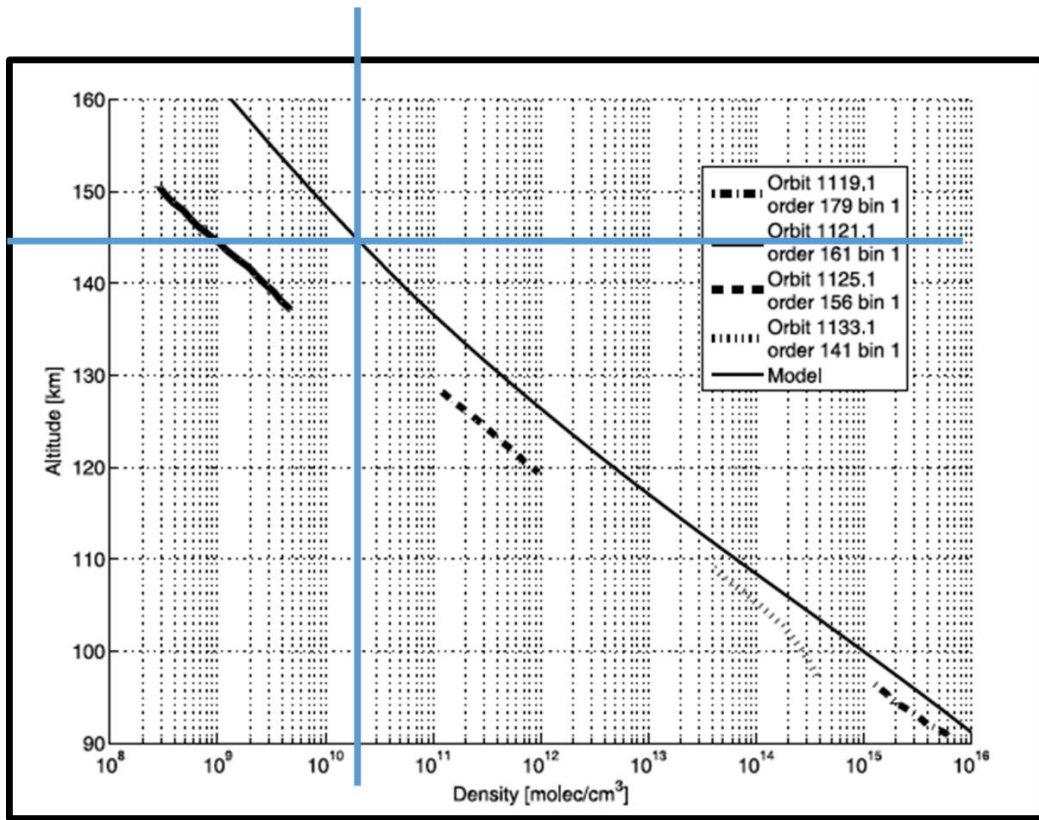


Figure 4. Reference atmospheric density at deployment altitude (shown in blue). From Mahieux et al. (2010)

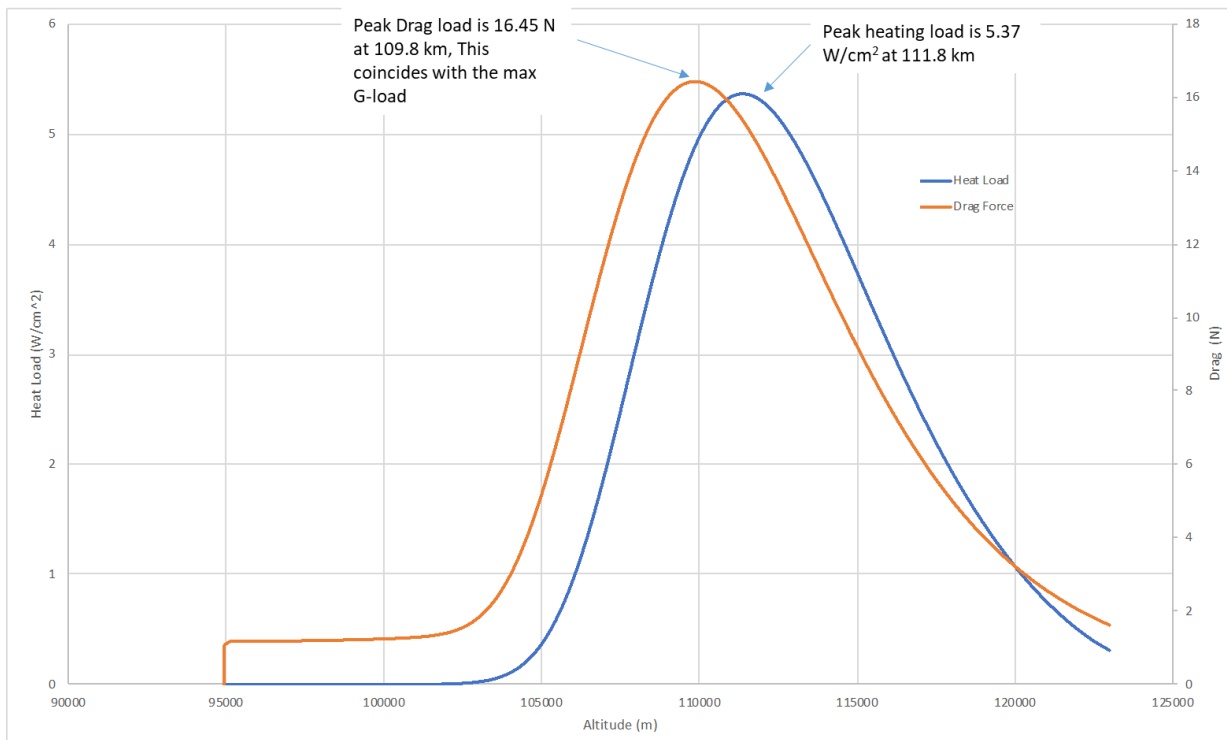


Figure 5. Peak load and heating from orbital entry simulation.

We used these results in conjunction with measurements of the zonal (along lines of latitude) wind velocity at relevant altitudes (Peralta et al., 2017), shown in Figure 6 to estimate the lateral drift distance, suspended lifetime in the target altitude range, and time from start of operations at 100 km to surface contact. In the absence of effects that could cause LEAVES units to descend faster or slower (i.e. convection and turbulence), we estimate that operational lifetime from 100 – 30 km is 560 minutes, with time to surface contact of around 2100 minutes (Figure 7). Using the Peralta et al. model of wind speed, we calculate a lateral drift distance of approximately 1500 km upon reaching 30 km altitude and nearly 3000 km upon surface contact (Figure 8).

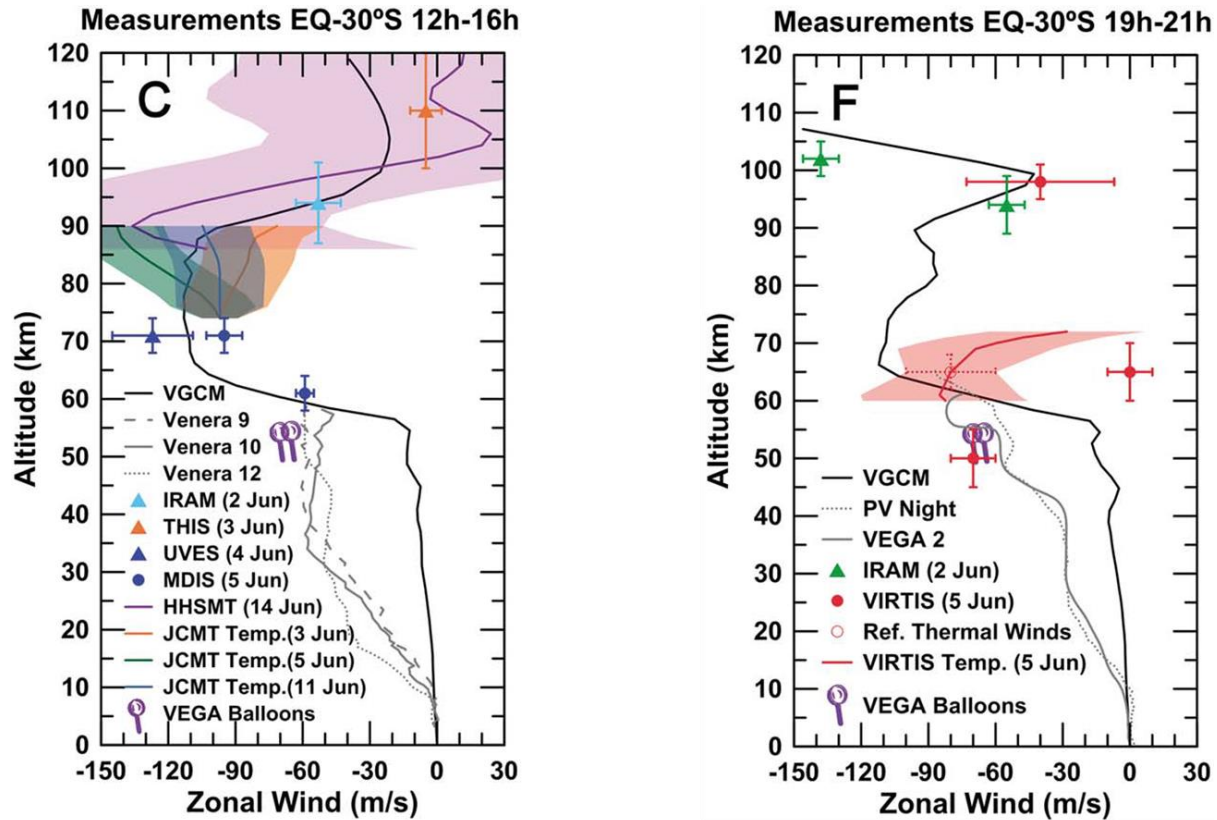


Figure 6. Zonal wind speed versus altitude. From Peralta et al. (2017).

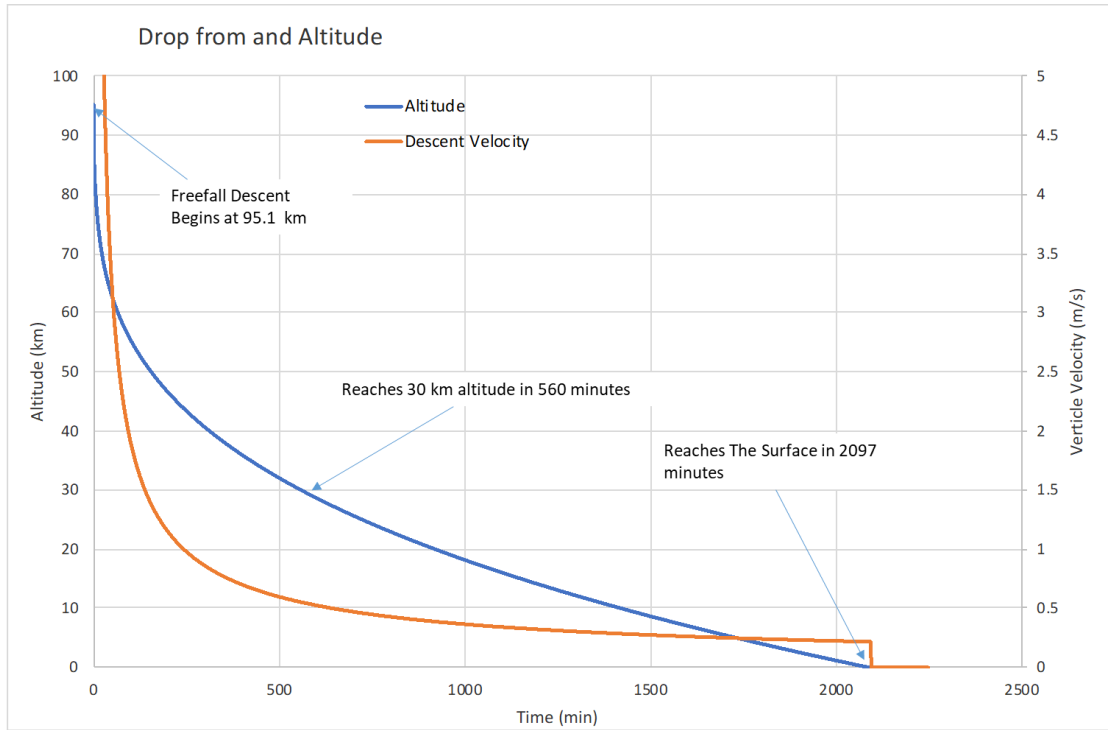


Figure 7. Duration of science operations and time to surface contact after start of operations

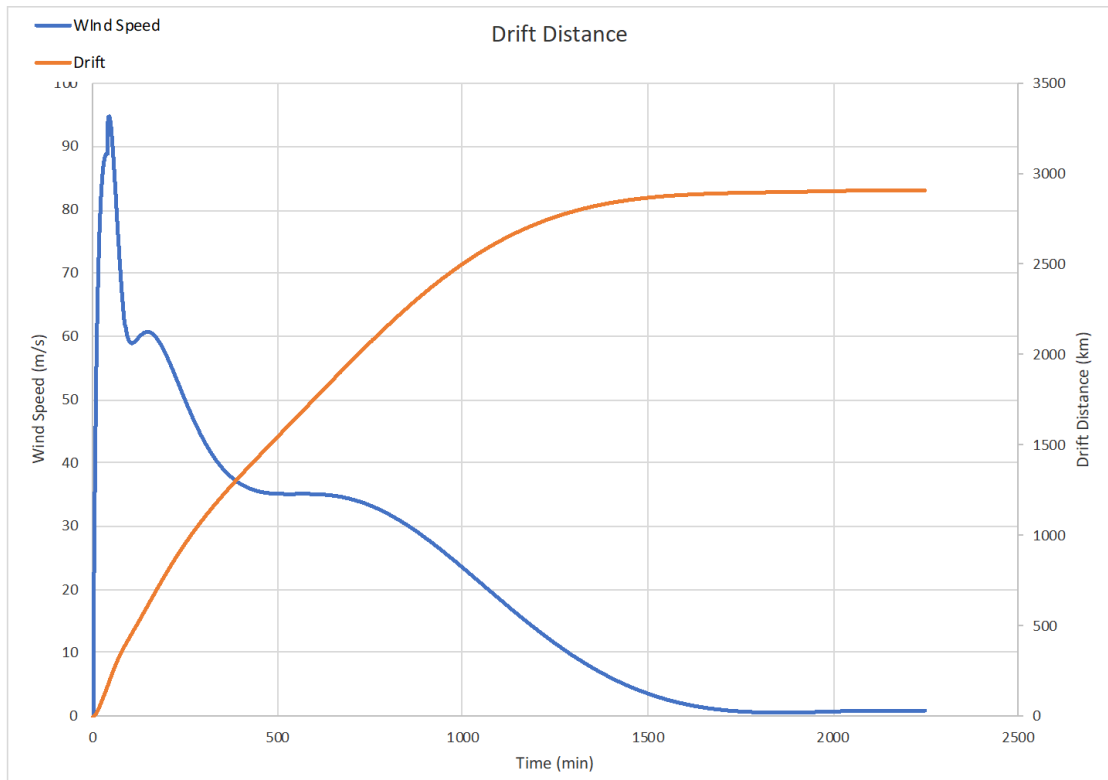


Figure 8. Lateral drift distance versus time from start of science operations

The results above were used to perform structural and thermal analysis to ensure that we did not exceed the tolerances of Kapton®. With a safety factor of 2, the allowable maximum stress for this material is 68 MPa (10,000 psi) at 200° C and maximum total temperature of 400° C (DuPont, 2017). For the carbon struts the maximum allowable stress is 300 MPa or 44,000 psi. Results of stress models are shown in Figure 9 and Figure 10. These models indicate that our chosen areal mass density of 0.126 kg/m<sup>2</sup> is appropriate for the load experience during nominal entry conditions at 145 km altitude and relative velocity of ~ 5 km/s. We note that the maximum stress experienced by the structural members is well below the maximum allowable stress, potentially allowing for flexibility in choosing other orbital conditions and adding resiliency to non-nominal deployment.

Loaded with 20 N, +y direction.

$\sigma_{\max} = 7.7 \text{ MPa (1.1 ksi)}$   
 $\sigma_{\text{allow}} = 68 \text{ MPa (10 ksi)}$   
 Margin: 8.1

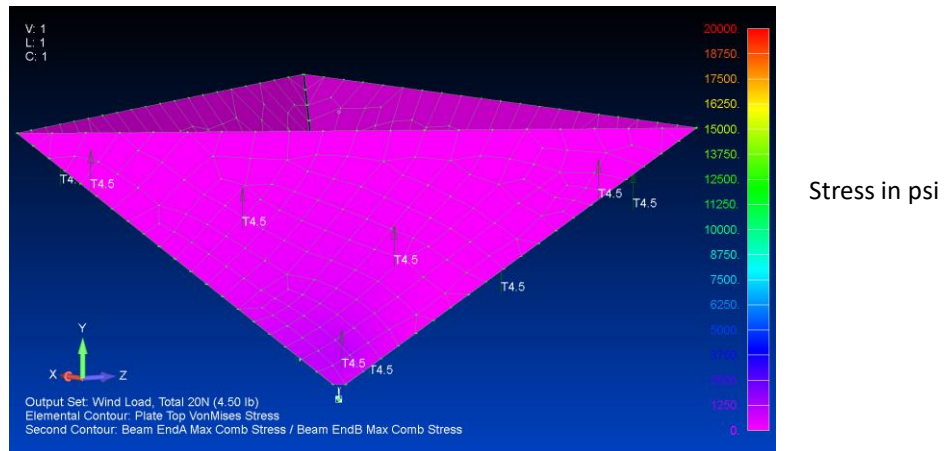


Figure 9. Finite element model of maximum stress on panels

Loaded with 20 N, +y direction.

$\sigma_{\max} = 94.3 \text{ MPa (13.7 ksi)}$   
 $\sigma_{\text{allow}} = 300 \text{ MPa (44 ksi)}$   
 Margin: 2.2

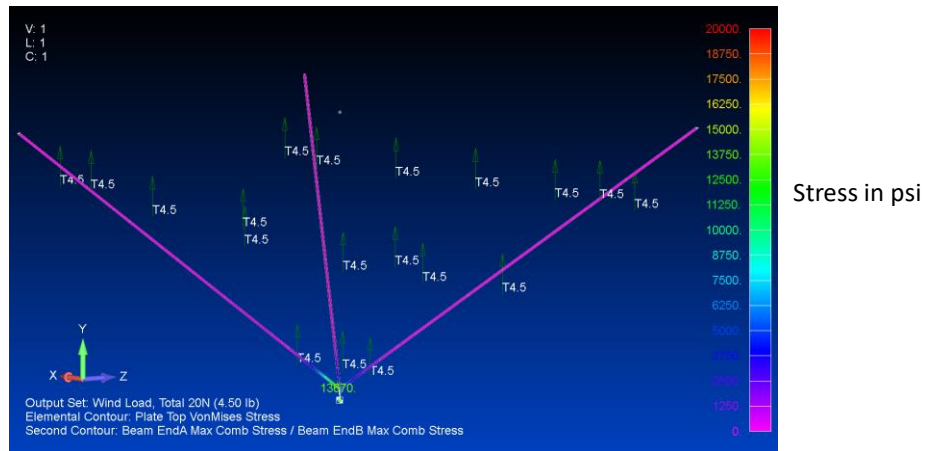


Figure 10. Finite element model of stress on carbon fiber struts

In order to maximize efficiency and lofted lifetime, we performed a sensitivity analysis that varied areal density (ratio of total mass to aerodynamic projected area), shown in Figure 11. It is worth noting that increasing surface area by scaling up the triangular panels causes the structural mass to grow faster than area. So, this sensitivity

analysis is an important optimization step. Our chosen areal mass density of 0.126 kg/m<sup>2</sup> was driven by the minimum mass of the payload. Table 1 indicates that a trade of increased payload mass for lower lifetime should be approached with caution due to the doubling of thermal heating (in this case, the primary failure mode) and maximum stress.

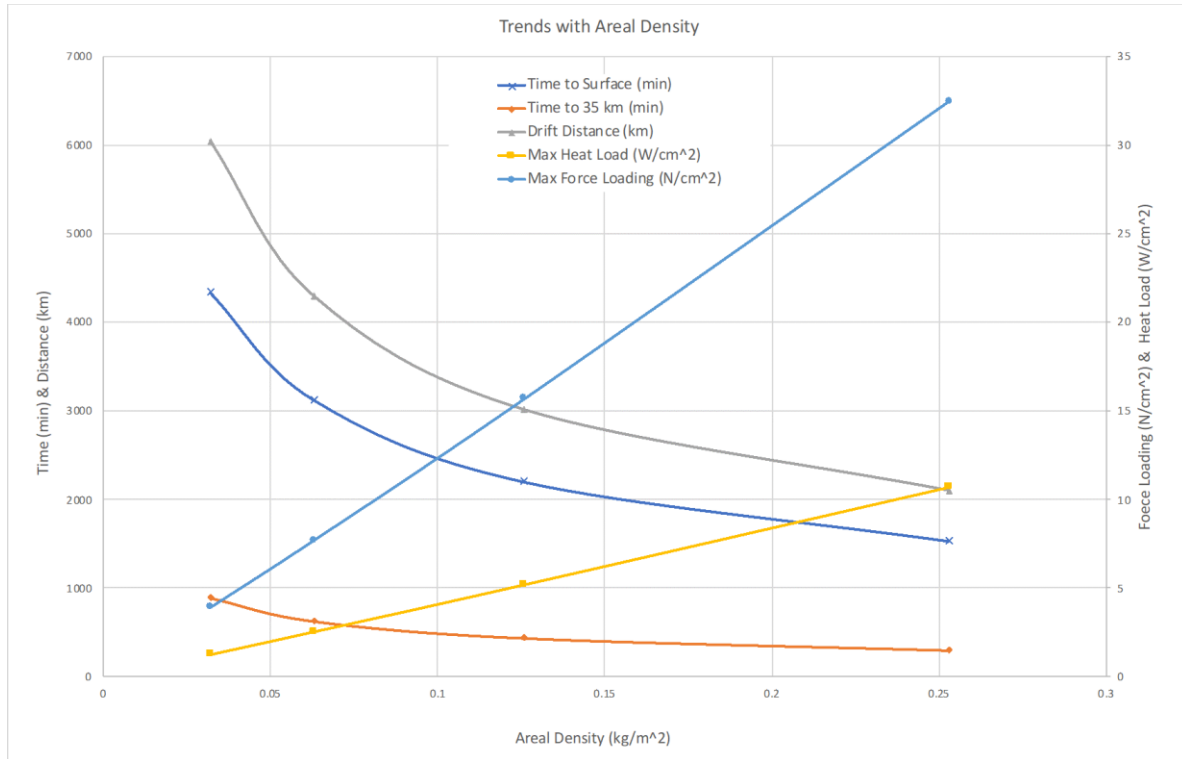


Figure 11. Sensitivity of deployment and descent conditions to areal density

Areal Density	Time to Surface	Time to 35 km Altitude	Drift Distance	Maximum Heat Load	Maximum Force Loading
0.032 (kg/m <sup>2</sup> )	4347 Min	891.0 Min	6056 km	1.25 W/cm <sup>2</sup>	3.9 N/m <sup>2</sup>
0.063 (kg/m <sup>2</sup> )	3130 Min	627.0 Min	4300 km	2.54 W/cm <sup>2</sup>	7.7 N/m <sup>2</sup>
0.126 (kg/m <sup>2</sup> )	2203 Min	436.8 Min	3014 km	5.20 W/cm <sup>2</sup>	15.7 N/m <sup>2</sup>
0.253 (kg/m <sup>2</sup> )	1533 Min	300.1 Min	2103 km	10.70 W/cm <sup>2</sup>	32.5 N/m <sup>2</sup>

Table 1. Summary of selected areal densities and resulting mission effects

One advantage of using rigid spars with flexible side panels is the ability to collapse one panel while pivoting one spar to lay over the other. This creates a flat-packing configuration as shown in Figure 12. This means that dozens, if not hundreds, of the LEAVES units can be compactly stored and integrated as a secondary payload on an orbiter mission. One such arrangement can be seen in Figure 13, where 100 units are packed into a 130 x 130 x 90 cm volume. In this study, we did not specify or design the deployment mechanism. We imagine that such a mechanism would take a form similar

to a mechanized card-dealer, with a cogging motor wheel that ejects the topmost LEAVES unit, while successive units are pushed to the top of the “deck” by a spring-loaded mechanism.

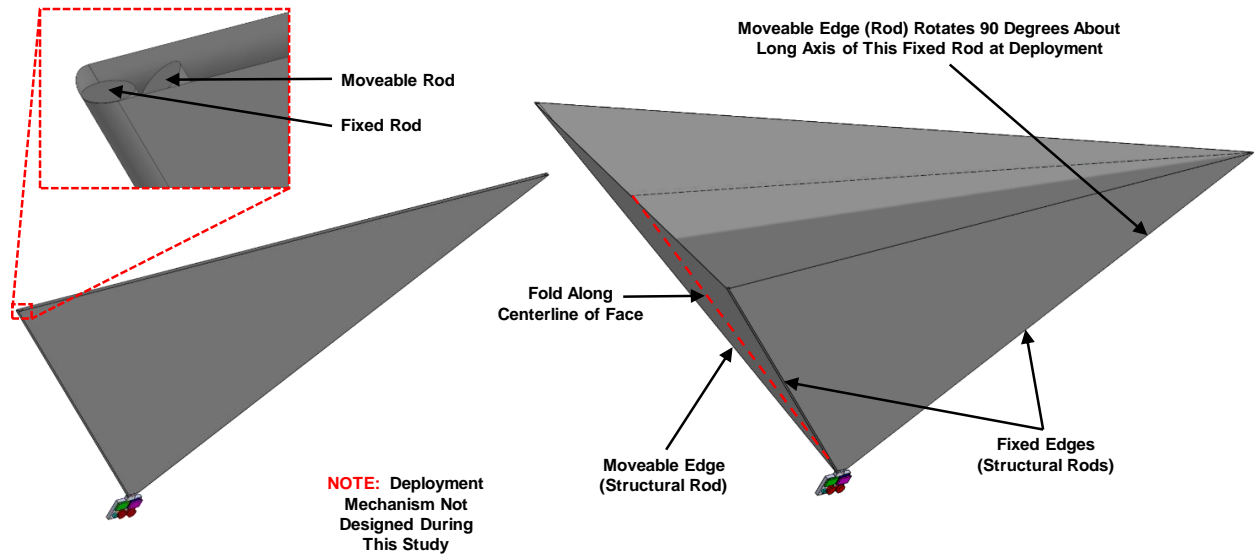


Figure 12. LEAVES flat-packed stowing concept

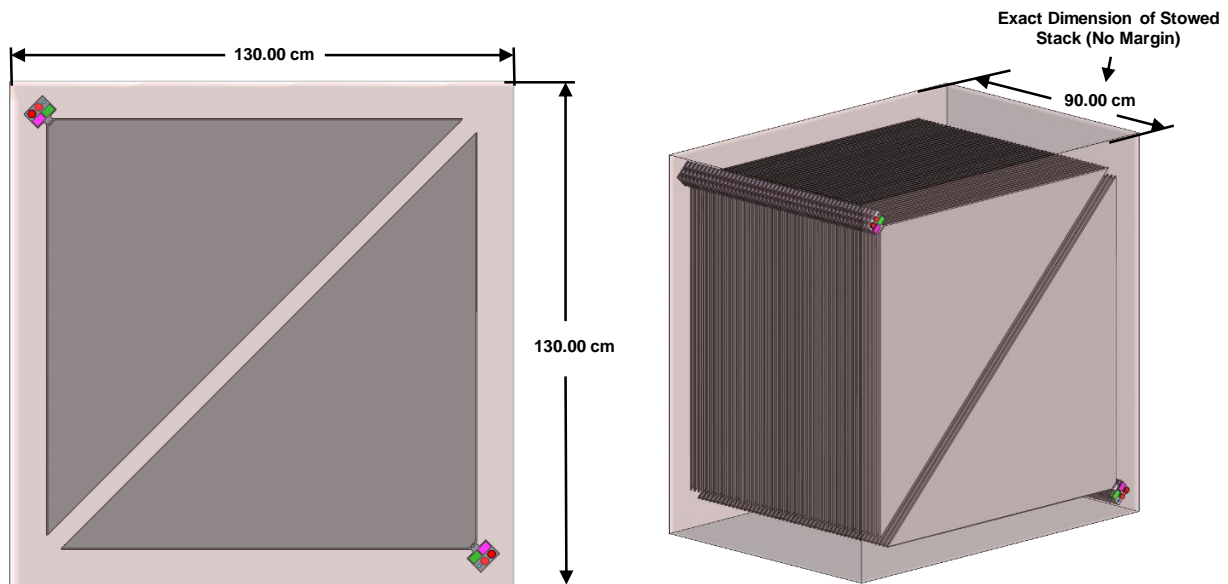


Figure 13. Compact stowed configuration of 100 LEAVES units

## 5.2 PAYLOAD OVERVIEW

The entire active payload (i.e. the powered portion) is housed in a rectangular assembly that is around only half the size of a modern mobile phone. Shown in Figure 14 are the two double stacks of coin cell batteries (red), processor and radio (green), inertial measurement unit (blue), and sensor assembly (violet).



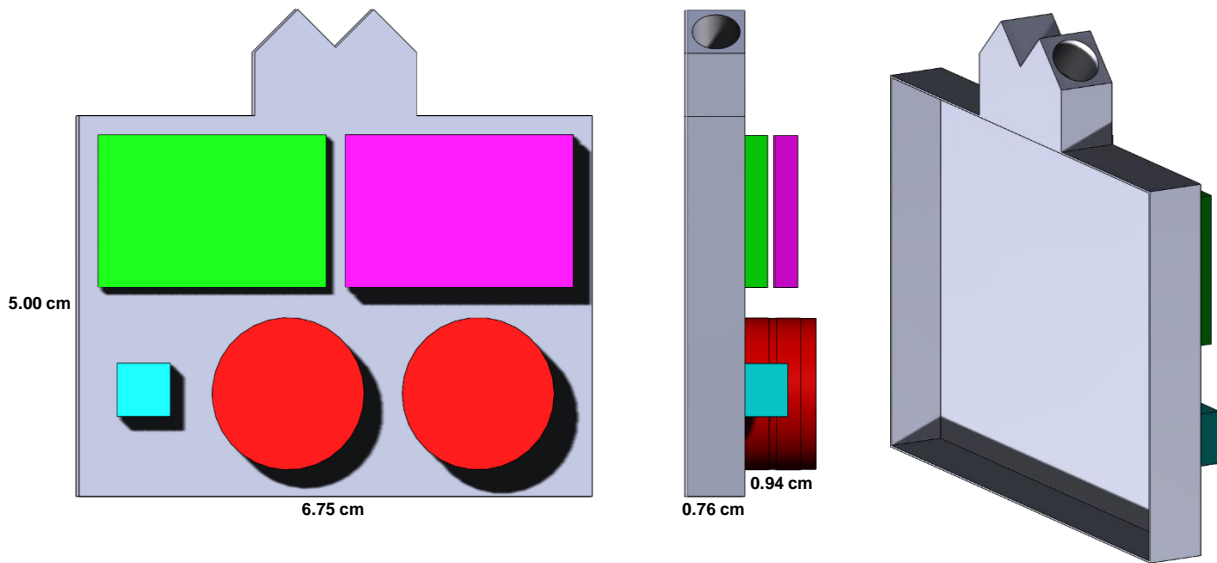


Figure 14. Powered payload configuration

### 5.3 SENSORS

A key enabling feature for LEAVES that differentiates it from heritage atmospheric probes is the miniaturization of both conventional electronics and sensors, and those designed to operate in the Venus environment. There are multiple options for science sensor configurations, with the most fundamental being temperature and pressure. While both data sets are useful for advancing knowledge of the Venus atmosphere, the pressure data can be used as a first-order altimeter by comparing with a reference atmospheric model (Kliore et al., 1992). Both sensors are available as off-the-shelf components, though the range of pressures that LEAVES will experience means that two pressure sensors will be needed. A low pressure sensor covering  $10^{-3}$  to 30 torr is available from Pirani and draws  $< 5$  mW. The second pressure sensor is widely available from different vendors and has a range of 30 – 7600 Torr (10 atm), with a power draw of  $< 3$  mW.

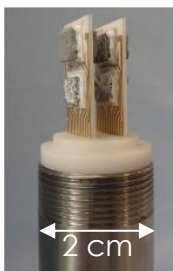


Figure 15. MEMS atmospheric sensor array. Credit - Makel Engineering, Inc.

Micro Electro-Mechanical Systems (MEMS) sensors for detecting chemical species with high resolution allow for a generational advance in understanding the chemistry and chemical variations in Venus' atmosphere. Silicon-carbide based semiconductor technology allows for stable operation to over  $500^{\circ}$  C without the need for thermal mitigation and is naturally highly resistant to the corrosive sulfuric acid clouds (Philip G. Neudeck et al., 2016). Sensors for both  $\text{SO}_2$  and  $\text{CO}$  have been developed and matured to TRL 6 by ongoing collaboration between NASA Glenn Research Center and Makel Engineering, Inc (G. Hunter, 2016; G. W. Hunter & Culley, 2012; Makel & Carranza, 2015). Leveraging existing data about the general chemical composition of Venus' atmosphere allows for the use of these highly specific sensors to achieve a sensitivity of better than 1 ppm, with a mass of  $\sim 1$  g, and

power requirements of a few tens of milliwatts. No COTS sensors exist (for SO<sub>2</sub> and CO) that offer comparable sensitivity, mass, and power needs. However, because the SiC sensors are designed to operate in conditions that exceed ~220° C (equivalent to ~30 km altitude), they must be actively heated. To maximize the use of a heated substrate, we chose to package a chemical species sensor on either side of the heater. At worst case (i.e. 100 km altitude at -105° C), the heated assembly, with sensor operation, will draw 35 mW. The table below shows a detailed list of the science payload:

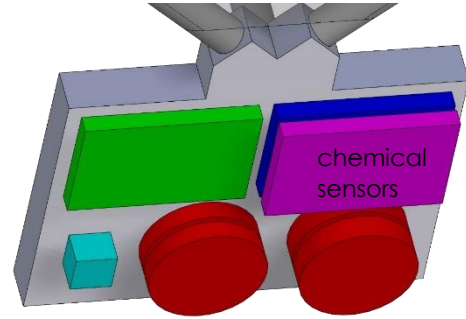


Figure 16. Location of chemical sensors on payload

	Mass (grams)	Max Power (mW)
Chemical Sensor Subassembly	2.5	35
Pirani Pressure Sensor	0.6	5 <sup>(a)</sup>
MEMs Pressure Sensor	0.5	3 <sup>(a)</sup>
Temperature Sensor	0.5	2
Substrate	1	
(misc, FET, OP AMP)	0.5	(b)
	5.6	42

(a) Only one on at a time with minimal overlap

(b) accounted for in sensor power budget

Table 2. Science payload mass and power budget

## 5.4 ELECTRONICS

COTS microprocessors, such as the Texas Instruments SM470R1B1M-HT are capable of functioning from -55° C to over 200° C and include 1 MB of program memory, 64 KB of flash memory, 12 analog-to-digital channels with 10 bit resolution, and dozens of general purpose I/O channels. This microprocessor is tasked with scheduling, communications, data acquisition and storage, and signal processing. The core of a Command and Data Handling unit (CDH) is formed when this microprocessor is combined with an industrial, high temperature (200° C) field effect transistor (FET), operational amplifiers (opamps), and a stabilized real-time oscillator clock. A functional schematic of the CDH system is shown below, where functions of the microprocessor are broken out as separate entities.

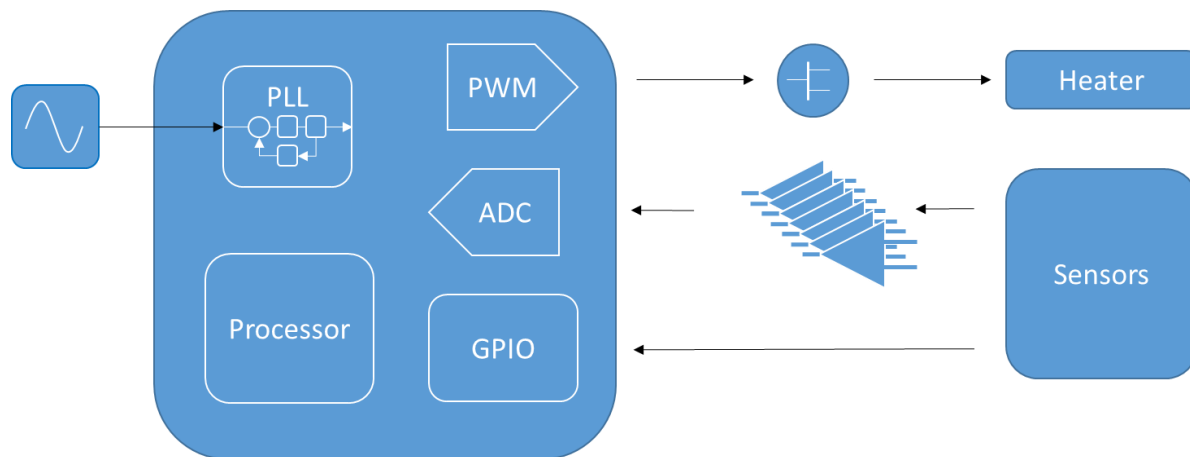


Figure 17. Command and data handling functional block diagram

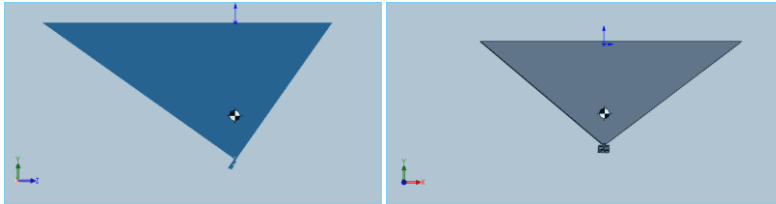
## 5.5 TRACKING AND GEOLOCATION

The problem of geolocating subspacecraft or probes in an environment where there is a dearth of fixed reference points is significant. Historically, entry probes were located using a combination of delay Doppler (for ranging) and modeled entry profile or Very Long Baseline Interferometry (VLBI). In both cases, position was determined after the entry campaign. Our original and preferred solution would have been to determine position based upon post-campaign data on the relative positions and velocities of each LEAVES unit from each other. This could have taken the form of inter-probe radio ranging combined with absolute altitude (from filtered pressure data) or derivation of distance through integration of continuous Inertial Measurement Unit (IMU) data on the state of acceleration and rotation of the probe.

We investigated the option for IMU-based location derivation by assuming that once the probe has reached an evolving state of terminal velocity, nadir and westward directions might be detectable as vertical and horizontal drag. These data would be filtered for asymmetric effects acting upon the probe by assuming that any imperfection in the probe shape would cause a rotation in the structure that acts approximately as a wind-driven clock. We required a 50 Hz sampling rate of the IMU in order to capture all components of probe motion. This sampling rate is near the maximum of the capability of our representation Command and Data Handling configuration.

Principal MOIs about CG

CG (cm) wrt frame shown below	$I_{xx}$ (gm*cm <sup>2</sup> )	$I_{yy}$ (gm*cm <sup>2</sup> )	$I_{zz}$ (gm*cm <sup>2</sup> )
(-0.4,-51.8,-0.5)	165711	168425	176412



- The CG is given in the frame shown. The z-x plane is coincident with the wide end of the pyramid
- The Principal Moments are given in the Principal Frame
  - Rotation about the  $I_{zz}$  axis (close to y-axis above) should result in periodic, conical motion of the payload in an inertial frame

Figure 18. Relative motion tracking assumptions

Naturally, as time progresses noise-based error will cause position uncertainty to accumulate. We performed a Monte Carlo simulation in order to constrain this uncertainty. We demonstrate in Figure 19 that 3 hours after start of operations, relative uncertainty can approach 25 km. Thus, we consider this approach to be reasonable if not ideal for determination of probe position, though continued error growth will almost certainly mean that relying upon this approach alone will result in poorly constrained location at the lower altitudes. An additional caveat is that absolute position must be constrained at the start of this integration.

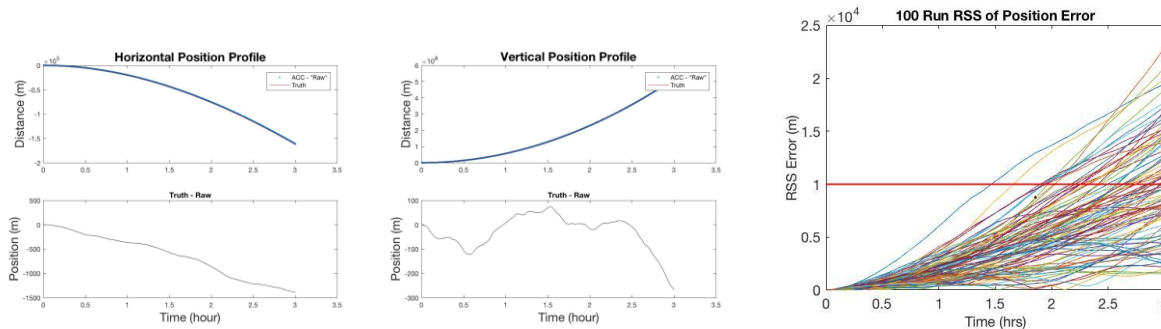


Figure 19. Demonstration of uncertainty in direct integration of position

There are likely a number of innovative solutions for arriving at a more robust determination of position for a sensor swarm, but the limited duration of Phase I study did not permit such exercises. Therefore, we opted to make it a requirement of the hosting orbiter to directly observe and locate, via S-band radar, the deployed LEAVES unit. Because the absolute position of the orbiter will be known from astrodynamics and

terrestrial tracking, we can combine these data with radar ranging and geolocation to constrain locations within our target of < 10 km resolution. (We note that this is well within the resolution of an S-band surface radar mapper.) We consider this to be a reasonable requirement of the hosting spacecraft since the total operational lifetime of the LEAVES units (during science operations) is ~9 hours, and the orbiter will need to act as a receiver-relay for the return of LEAVES instrument data. Orbital configurations, footprints, and viewing windows are discussed below. As indicated above, configuring the LEAVES structure to act as a cube-corner retroreflector allows for reflection of incident radar directly back to the orbiter.

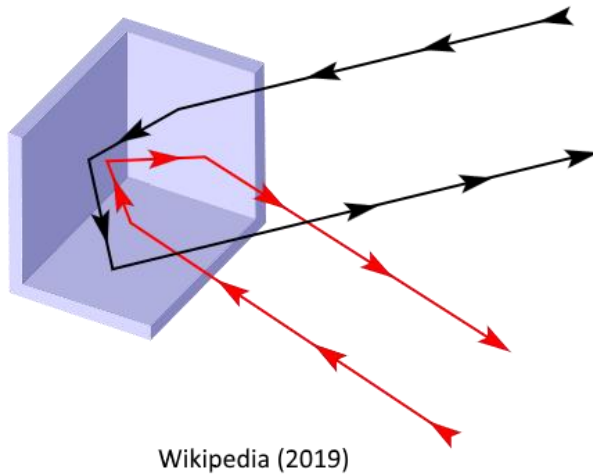


Figure 20. (Left) Illustration of parallel reflection via triple orthogonal redirection. (Right) Array of corner retroreflectors at the Nevada Test Site.

We analyzed a notional orbital radar geometry (Figure 21) with the orbiter at a range of 6000 km from a single LEAVES unit. We assume a 10 GHz pulse, with 80-90% return to the orbiter, signal-to-noise ratio of 4.5 dB and 2 s pulse integration. Figure 22 shows details of the radar geometry analysis. We compute effective antenna gain as:

$G = \frac{4\pi\sigma}{\lambda^2}$  where  $\sigma$  is effective radar cross section area (Figure 22), and  $\lambda$  is radar wavelength.

$G_t$  and  $G_r$  (gain of the transmitter and receiver antennas) are then used to compute:

$$\text{Received signal at the LEAVES unit} = \frac{P_t * G_t * G_r * \lambda^2}{(4\pi R)^2} = -72.6 \text{ dBW (based on 10 W Tx power)}$$

$$\text{Reflected signal from the LEAVES unit} = \frac{P_t * G_t * \lambda^2 * 4\pi\sigma}{(4\pi R)^2 * \lambda^2} = -78.6 \text{ dBW}$$

$$\text{Received signal from LEAVES unit} \approx -111.87 \text{ dBW or } -81.87 \text{ dBm}$$

Our conclusion is that the reflected signal from each LEAVES unit, when illuminated by a radar orbiter is sufficiently within a typical sensitivity of  $\approx -100$  dBm to make radar tracking a viable solution to geolocation.

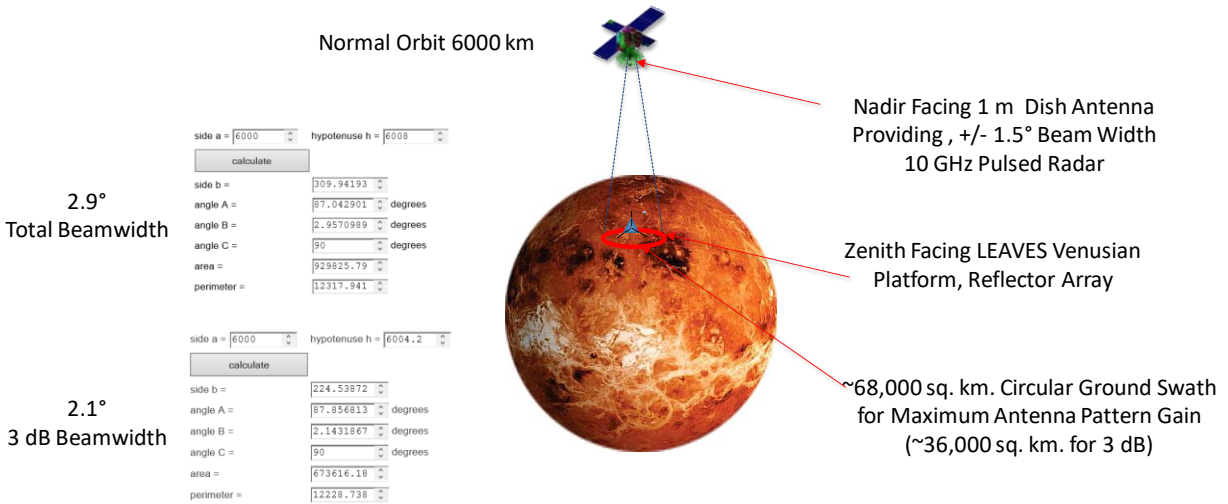


Figure 21. Illustration of radar tracking study

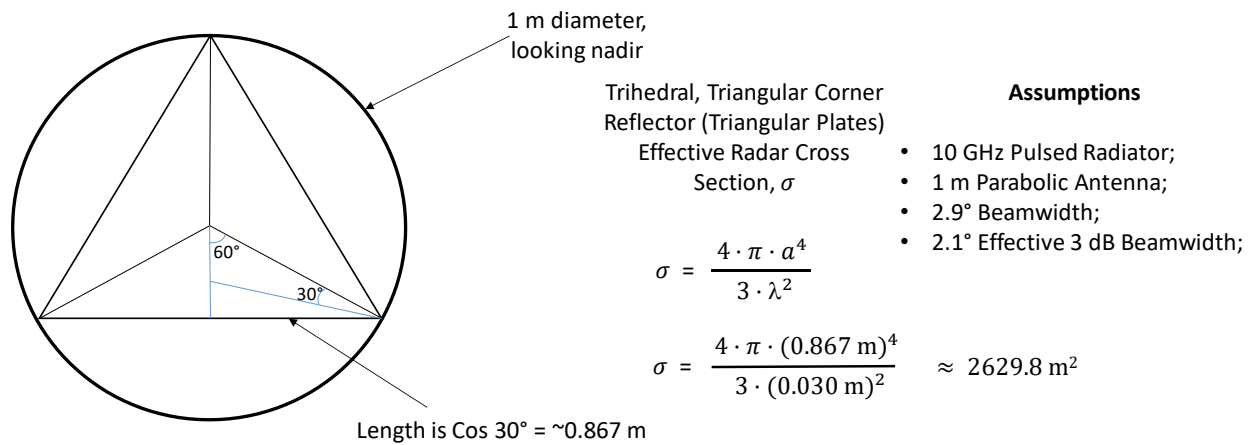


Figure 22. Radar geometry analysis

In the unlikely case that two or more LEAVES lie along the same radar ray path from the orbiter (Figure 23), processed and reduced IMU data may be used to uniquely distinguish between probe units. Used this way, positioning becomes a hybrid combination of relative and absolute positioning.

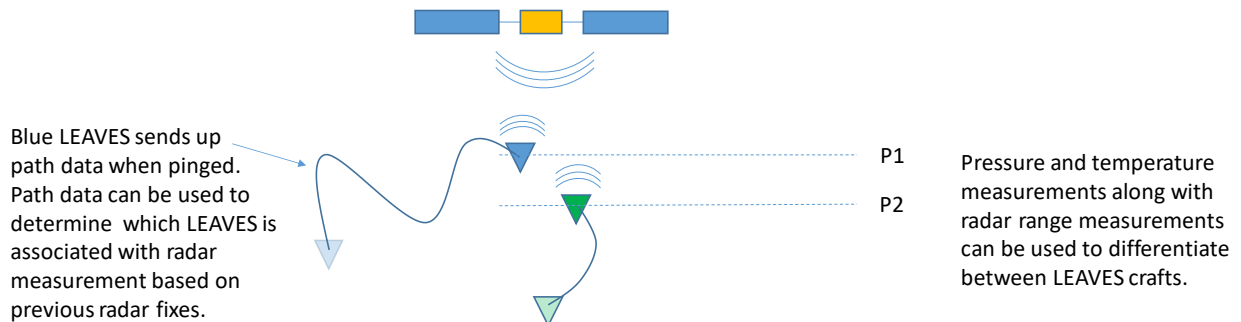


Figure 23. Coincident probe locations along radar ray path

## 5.6 COMMUNICATIONS

Key to conserving battery utilization (and therefore, total mass) is operating a ~1 W radio in transmit-only mode. We further conserve power by operating this radio using a preset timer or trigger based upon illumination by the host orbiter's tracking radar. The solution of a radar-based trigger is invoked, but not explicitly designed, in this study. Figure 2 shows the structural location of a full-wave, horizontal, dipole antenna that extends from one of the three corners to the midpoint of the opposite edge. A UHF microtransmitter, operating at 433 MHz with 0.6 W is driven by the microprocessor. As above, we assume a notional link range (i.e. distance between LEAVES unit and orbiter) of 6000 km. For the full-wave dipole, we assume a transmitter antenna gain of 3 dBi and a receiver antenna (aboard the orbiter) gain of 11 dBi. Our radio link budget analysis results in a data bandwidth of ~3.8 kbps (Figure 24). A 3-dimensional RF analysis was completed for preliminary inspection of the interaction between antenna, radio, and reflective panels, as seen in Figure 25.

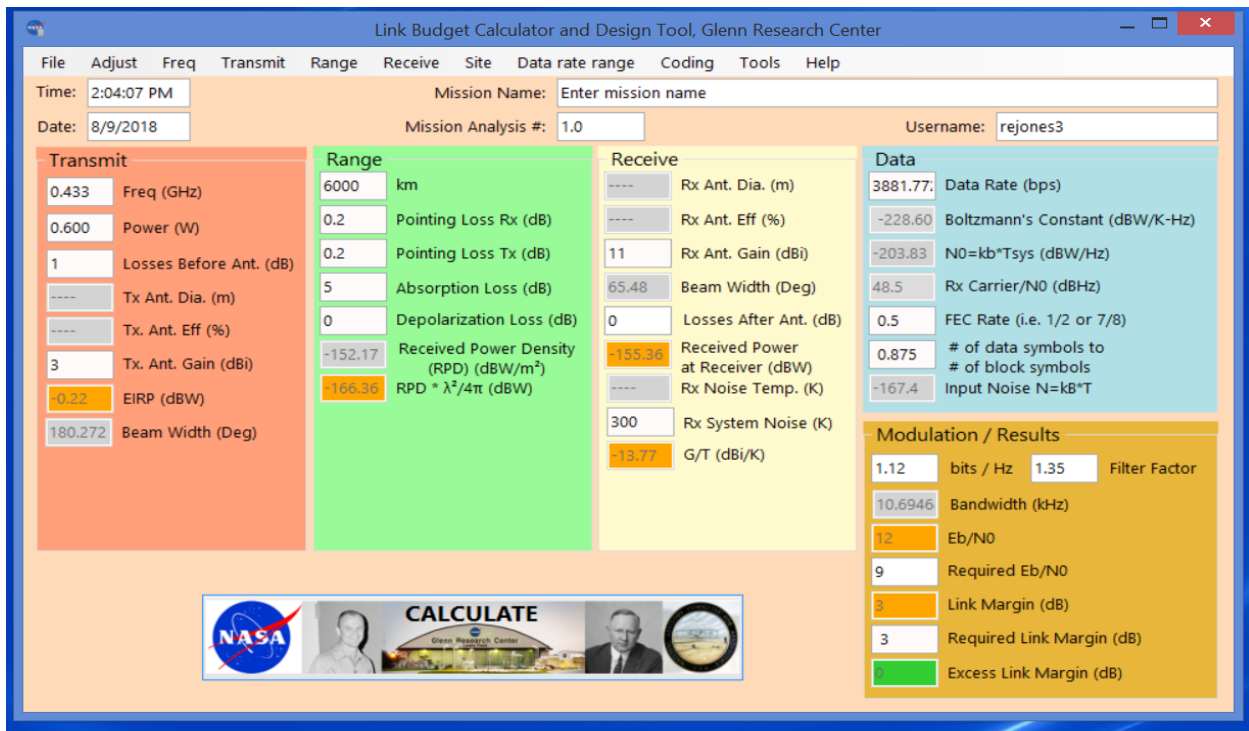


Figure 24. Radio link budget analysis

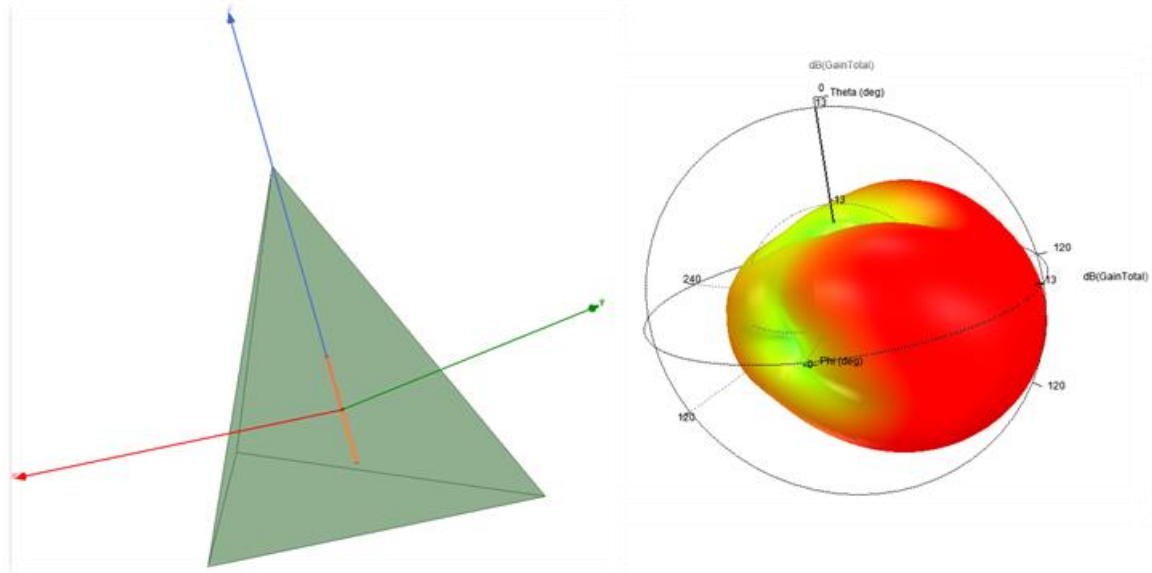


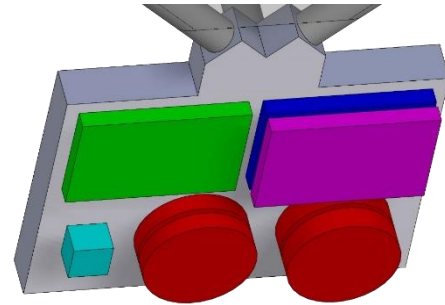
Figure 25. Radio radiation pattern analysis

In order to constrain data return rates and volumes, we use the 3.8 kpbs transmitting data rate shown above, with a total of 80 bps of data generated continuously from the round-robin sampling of IMU, physical, and chemical sensors. This means that over the 560 minute science mission duration, 2,688,000 bits of data will be generated. Data are cached and transmitted starting with the most recent data, and once the end of the cache is reached, the timestamped data are retransmitted for as long as the orbiter is in view. At the worst case (i.e. transmitting the full cache) these data will require ~11.8 min. Given that we expect each LEAVES unit to be viewed by the orbiter 4 times, we anticipate a total of 47 minutes transmit time. We note that while 0.336 MB is well under the limit for microprocessor program memory, the power requirements (and therefore battery mass) will be driven mainly by radio operations. Our design target was to complete one full cache transfer within 6 minutes (for 24 minutes of total transmit time), so this overrun is easily mitigated by introducing a brief sleep cycle between data acquisition cycles. Because a continuous acquisition of data far oversamples the required resolution of  $.1 \text{ km}^{-1}$ , we are confident that reducing sampling rate will have no effect on mission requirements.



## 5.7 POWER

An *a priori* requirement for the LEAVES power budget is that the maximum power draw at any given time must be no more than ~1 W. This means that power generation can reasonably be handled by batteries, supercapacitors, or even small solar panels. With over 100 W/m<sup>2</sup> available in nearly all of the target altitudes (Titov et al., 2013), solar power is an obvious solution. Utilizing thin film, flexible amorphous silicon panels with an efficiency of 5% would yield plenty of power for our application. However, LEAVES is required to operate in solar night as well as day. This means that a solar power solution incurs an additional penalty of voltage regulator, charge controller, and rechargeable battery. Because of the relatively limited lifetime of LEAVES (~ 9 hours), we found that non-rechargeable, coin cell batteries offer the best mass/power balance.



Power System shown in red.

In order to conserve power consumption, we operate in two primary modes: science data acquisition, and communications. During data acquisition, the science payload is operated continuously, with a power draw (including subsystems) of 0.17 W. With an operational lifetime of 576 minutes, the total power requirements for science operations is 1.63 W-hr. During communications, LEAVES requires 1.55 W for approximately 6 minutes. (Each of these estimates includes 30% growth margin.) With a nominal of 4 uplink events, the total power requirement for the communications subsystem is 0.62 W-hr. A Powered Equipment List, with growth margin, is shown below:

Description	Power Mode 1	Power Mode 2
Case 1 Study Name CD-2018-156	Science Operation, No Comm	Communicating, No Science
	576 min	24 min
	(W)	(W)
<b>LEAVES</b>	<b>0.1312</b>	<b>1.1918</b>
Leaf	0.1312	1.1918
Science	0.0450	0.0000
Attitude Determination and Control	0.0350	0.0350
Command & Data Handling	0.0500	0.0500
Communications and Tracking	0.0000	1.0000
Electrical Power Subsystem	0.0012	0.1068
Structures and Mechanisms	0.0000	0.0000

<b>Bus Power, System Total</b>	0.1312	1.1918
<b>30% growth</b>	0.0394	0.3575
<b>Total Bus Power Requirement</b>	<b>0.1706</b>	<b>1.5493</b>
<b>EP System power, System total</b>	0.0000	0.0000
<b>5% growth</b>	0.0000	0.0000
<b>EP System total Requirement</b>	<b>0.0000</b>	<b>0.0000</b>
<b>Total System power with growth</b>	<b>0.1706</b>	<b>1.5493</b>

Table 3. List of powered equipment

Thus, the total power requirement for each LEAVES unit is 2.25 W-hr. Conventional lithium coin cell batteries are capable of meeting this demand. A single CR2032 cell from Energizer supplies 235 mAh at 3.0 v. However, the maximum operating temperature of the CR2032 is 60° C. Because a primary requirement is to avoid active high temperature protection, we adopted a hybrid battery approach. Available lithium thionyl cells from Electrochem Solutions have an operating range of 70 – 200° C, with an energy density of ~0.741 W-hr/cm<sup>3</sup>. Scaling to the same size as the CR2032 results in a cell capable of supplying 266 mAh. The total power payload consists of two CR2032 cells and two lithium thionyl cells, operated sequentially as the LEAVES units falls through the atmosphere.



Figure 26. Electrochem MR Series

The total mass of this system (with ~40% growth) is 25 g, which includes batteries, a high temperature voltage regulator (i.e. Texas Instrument, Inc. TPS76901) and wiring harness. We note that while the Energizer CR2032 cells have flown in LEO (and we consider them to be TRL 6 at least), the lithium thionyl batteries are currently at TRL 3 with performance not yet proven in the relevant physical and chemical environment of the Venus atmosphere. Details of the power system payload are shown in the table below.

Description	QTY	Unit Mass	Basic Mass	Growth	Growth	Total Mass
<b>Case 1 LEAVES CD-2018-156</b>						
<b>Electrical Power Subsystem</b>			<b>0.0173</b>	<b>41.9%</b>	<b>0.0073</b>	<b>0.0246</b>
<b>Power Management &amp; Distribution</b>			<b>0.0053</b>	<b>46.2%</b>	<b>0.0025</b>	<b>0.0078</b>
Harness	1	0.0043	0.0043	50.0%	0.0022	0.0065
Voltage Regulator	1	0.0010	0.0010	30.0%	0.0003	0.0013
<b>Energy Storage</b>			<b>0.0120</b>	<b>40.0%</b>	<b>0.0048</b>	<b>0.0168</b>
Low Temperature Battery	2	0.0030	0.0060	30.0%	0.0018	0.0078
High Temperature Battery	2	0.0030	0.0060	50.0%	0.0030	0.0090

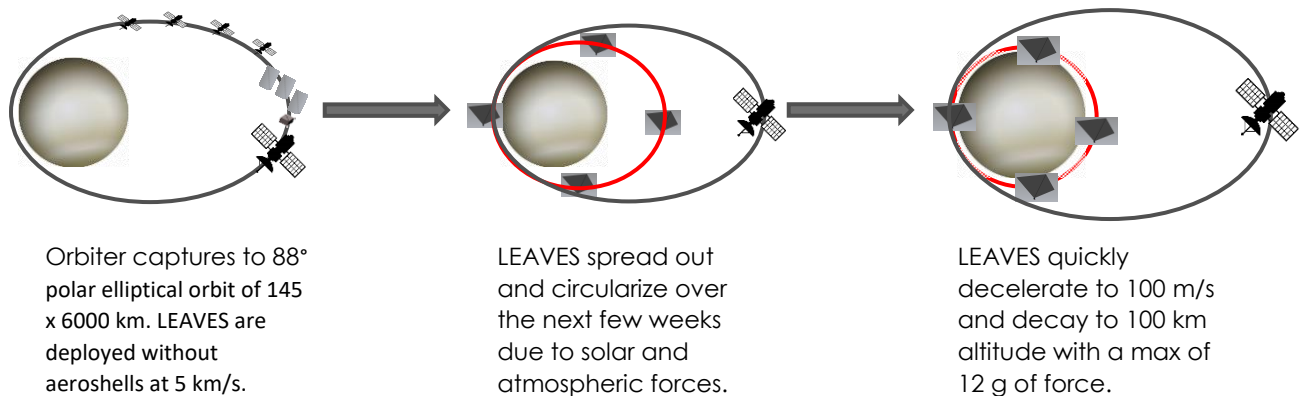
Table 4. Electrical Power Subsystem details

## 6 SWARMING VENUS – DESIGN REFERENCE MISSION

LEAVES is designed to be carried aboard, and deployed from, a primary, Venus-targeted orbiter. It is likely that near-future missions will involve a new generation of radar mapper (Hensley, Smrekar, Mueller, Helbert, & Mazarico, 2016), which would provide the necessary orbital configuration and infrastructure to support the LEAVES payload. Given the small mass (~ 130 g), we assumed a total of 100 LEAVES units could be carried as this payload as deployed as cohorts, in order to target different geographic regions or times during the solar day.

### 6.1 LAUNCH TO DEPLOYMENT

During the aerobraking campaign of the host spacecraft (L+5 to L+14 months for VERITAS), LEAVES are deployed from their stowed, flat-packed configuration in cohorts of ~20. From the deployment altitude of 145 km, the probes spring open and slowly decay to their target science altitude of 100 km.



#### 6.1.1 Entry Dynamics

The rate at which LEAVES units can be stably captured by the atmosphere (without exceeding maximum force or heating) is dependent on the altitude of periapsis of the orbiter, the relative velocity at the time of deployment, accurate knowledge of the atmospheric density at the deployment locations, and solar pressure effects. We estimate the time to circularize the LEAVES probes, after deployment, by using an analytical equations to calculate the  $\Delta V$  during each pass through the atmosphere (Forget & Capderou, 2010):

$$\Delta V = k \cdot \rho \cdot v^2 \cdot r_p \cdot (2\pi/\mu)^{1/2} \cdot (H/e)^{1/2}$$

Where:

$k = 0.5 \cdot (\text{ballistic coefficient}) = 0.5 \cdot (C_d \cdot \text{refArea}/\text{mass})$  and  $C_d$  is drag coefficient

$\rho$  = atmospheric density at  $H_p$

$v$  = relative speed (between vehicle and wind) at  $H_p$  (upper atmosphere winds assumed 100 m/s westward)  
 $r_p$  = periapsis radius  
 $\mu$  = planetary standard gravitational parameter  
 $e$  = orbit eccentricity  
 $H$  = planetary, atmospheric scale height (15.9 km)

After the  $\Delta V$  is calculated, the LEAVES orbit apoapsis is lowered accordingly. This process is repeated until eccentricity is less than 0.03. The  $\Delta V$  calculated for each iteration was on the order of 10s of m/s. We note that this equation is expected to be valid for Venus, though it has only thus far been validated for Mars.

The results of a suite of models, with periapses ranging from 140 km to 120 km is shown below. We concluded that LEAVES altitude decay time can be tuned (from hours to weeks) by targeting specific deployment altitudes. Moreover, a periapsis of <120 km results in rapid entry with excessive force and heating, while > 145 km may result in no atmospheric capture at all.

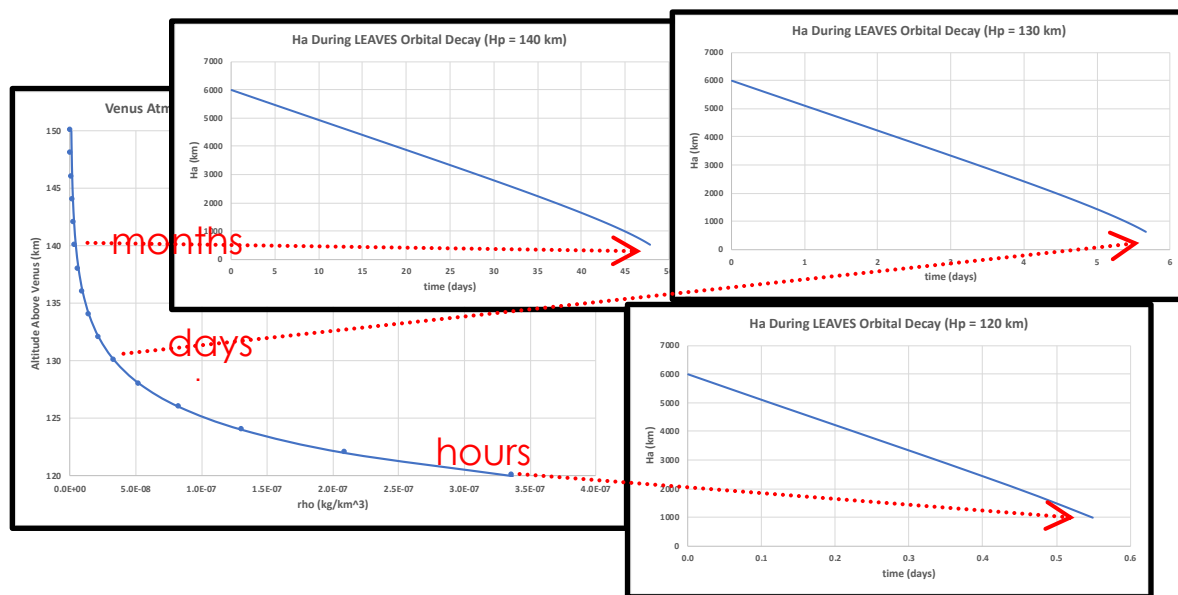


Figure 27. Comparison of orbital decay times versus deployment altitude

## 6.2 SCIENCE OPERATIONS

After reaching their target altitude of 100 km, the LEAVES units are activated by a barometric switch. Each probe is carried westward by the upper atmospheric winds at  $\sim 100$  m/s. The expanded structure of the probes acts as radar retroreflector, allowing (and requiring) active tracking by the orbiting satellite during the  $\sim 9$  hour descent to 30 km of altitude. Each unit continuously records temperature, pressure, 9-axis inertial state,  $\text{SO}_2$  and CO concentration in a round-robin sampling approach. These cached and timestamped data are transmitted in whole to the orbiter periodically along with the unit identification code, starting with the most recent data. Although the probes are drifting westward, they remain in the viewable footprint of the orbiter when it passes overhead. Because the orbiter remains in a near-polar orbit, each probe will get multiple "looks" during the descent.

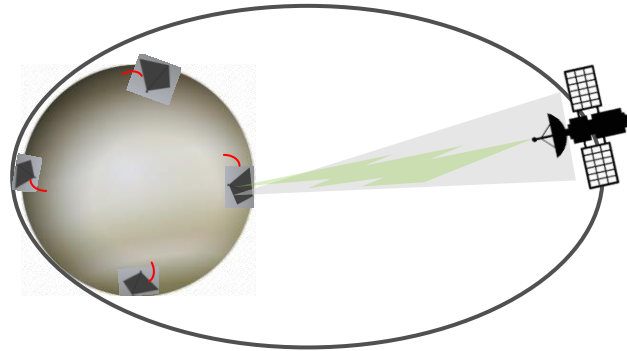


Figure 28. Illustration of relationship of deployed LEAVES to orbiter during science operations

Analysis of the relationship of the orbiter to the deployed LEAVES probes was conducted with the Satellite Orbit Analysis Program (SOAP), using our baseline orbiter configuration with a periapsis of 300 km and apoapsis of 6000 km. The footprint at each extreme, with a sensor half-angle of  $\pm 60^\circ$  is shown in Figure 29. Due to the narrowing footprint between periapsis and apoapsis, and the westward drift as they are carried on the zonal winds, each probe will experience a different contact duration. Most units will have 4 contact opportunities lasting at least 10 minutes, with a very few number of units (those under the periapsis) having no contact (Figure 30). Each series of LEAVES (i.e. "cohort") deployed approximately along lines of longitude, are expected to cover approximately 4 degrees of longitude, owing to zonal wind drift, before reaching their nominal terminal altitude of 30 km. By deploying multiple cohorts, LEAVES can sample an exceptional range of locations and depths within Venus' atmosphere.

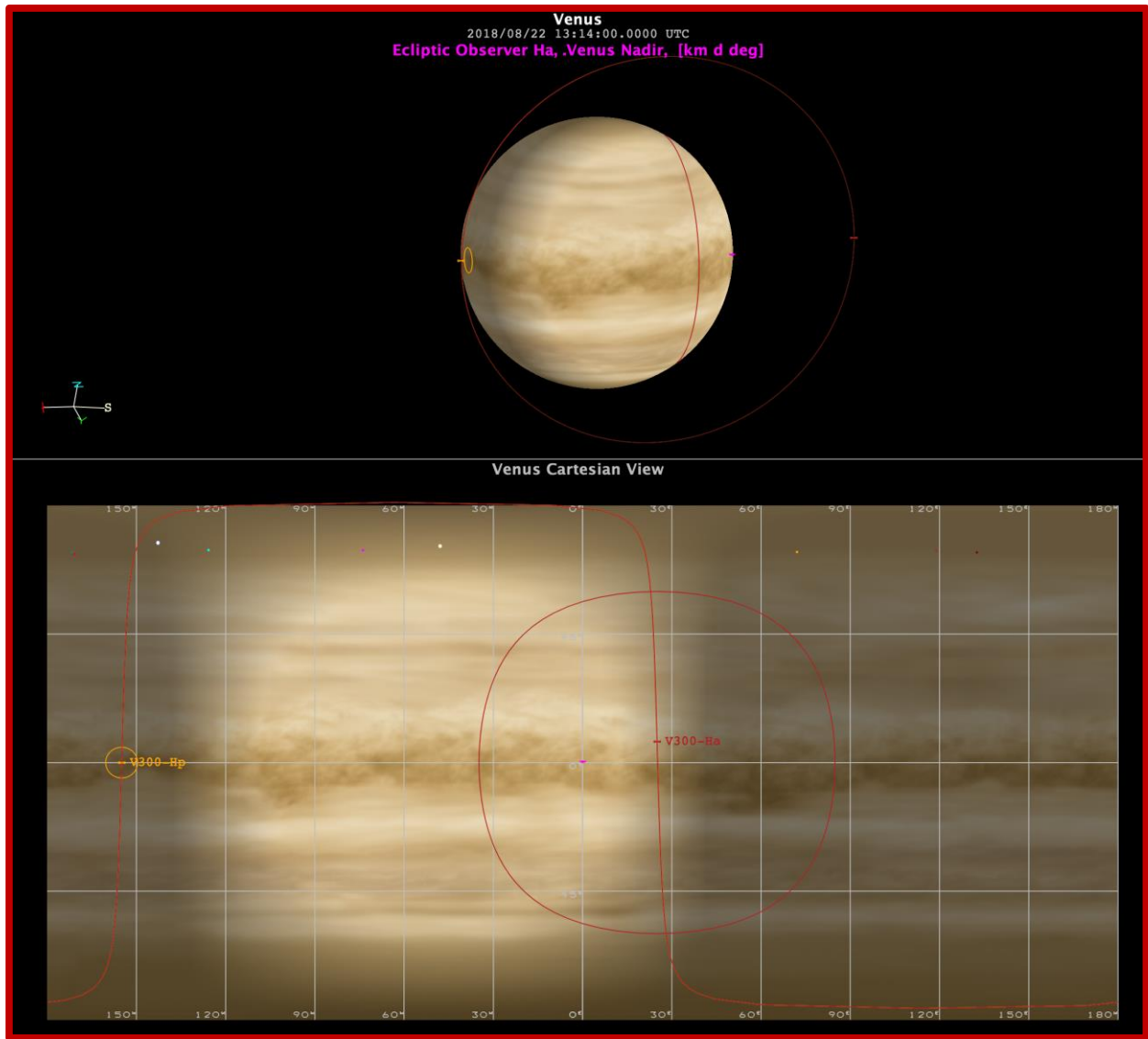


Figure 29. Orbiter radar footprint

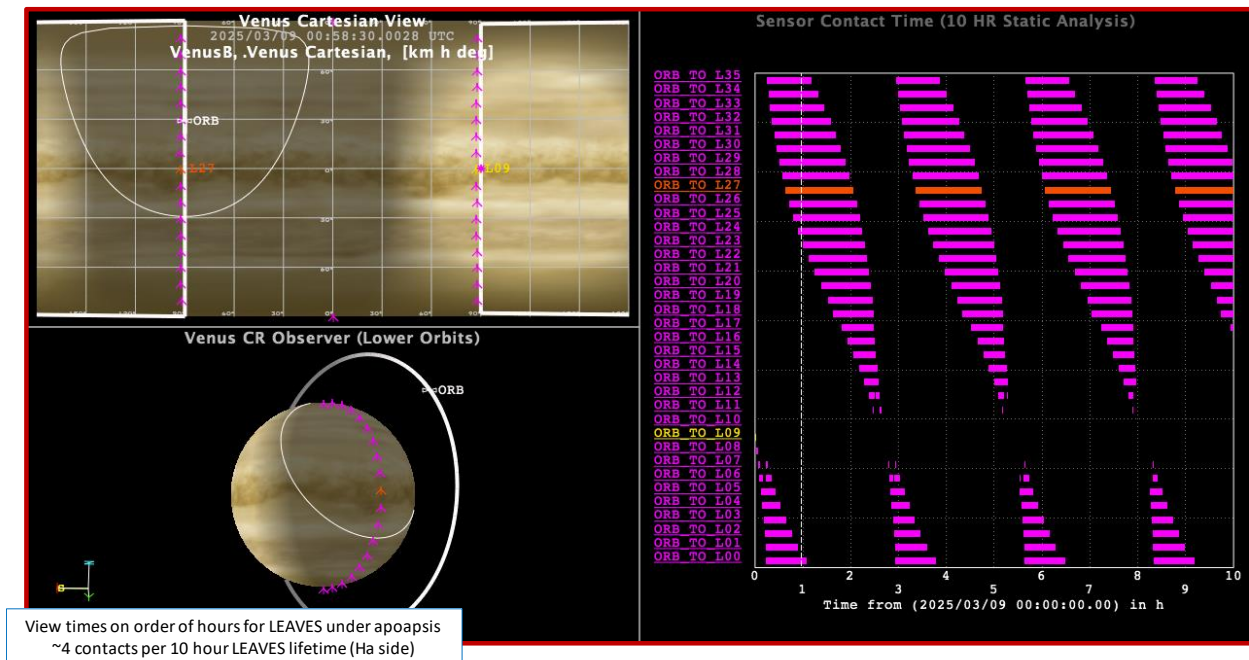


Figure 30. Optimized orbital configuration for LEAVES radio contact and tracking

## 7 PERFORMANCE TRADES AND OPTIONS

### 7.1 OPTIONS FOR MISSION EXTENSION

After the conclusion of our main study, which showed that the LEAVES concept is a viable and novel mode of atmospheric investigation, we conducted a limited follow up exercise to determine how deep in Venus' atmosphere the probes could function. There are several motivations for extending the operational depth: 1) atmospheric chemistry is progressively less constrained under the clouds and nearer to the surface, and 2) the increased density of the atmosphere means that the probe sink rate slows appreciably and extends the suspended lifetime nearly linearly by around 50 min/km below 30 km altitude. We investigated two possible cases for mission extension: 1) operation to 20 km altitude, and 2) operation to the surface.

#### 7.1.1 Option 1 – Full science operation

Continued operation below 30 km (above 225° C) requires a shift to components electronics components that are less mature and more specialized for high temperature environments. While the SiC chemical species sensors are fully capable of operating in an thermal environment down to the surface, there is currently no equivalent of a SiC, GaN, or other alternative, wide bandgap microprocessor available for these purposes. However, silicon-on-insulator microcontrollers have been produced with a manufacturer-derated performance up to 300° C. A caveat to this approach is

that the microcontroller lacks the speed, memory, and I/O of the microprocessor. This means that each of the missing components would add mass and power to the total payload.

Due to the 50% increase in operational lifetime, data storage requirements increase to 1.5 MB, exceeding that available even in the original microprocessor. At a minimum, power requirements would increase a corresponding amount, but a switch to sodium sulfur or sodium-nickel-chloride batteries reduces the energy density by 50%. This ultimately increases the battery mass by 12 g.

Communications could be enabled by 100 MHz SiC MESFET produced by Cree, Inc. which has been demonstrated to function for up to 72 hours at 475° C. It is not known whether this chip is still commercially available, however.

Extending the LEAVES model even 10 km deeper into the atmosphere presents significant but not insurmountable challenges. Some variation of the existing model, with higher mass and reduced capability (e.g. a lower sampling rate communications frequency) might be able to be constructed, but this approach will likely result in structural modifications and changes to the aerodynamic profile. This means that re-design of the platform would be needed in order to retain the ability to perform unshielded atmospheric entry.

### **7.1.2 Option 2 – Surface Survivability**

Where Option 1 examined the ability to continue to perform science operations into the deeper atmosphere, Option 2 focuses on the ability of the structure to survive descent to the surface. Because we have chosen a structure (inverted pyramid) that acts as a radar retroreflector, the ability to track each individual LEAVES unit to the surface would still yield valuable science about locally- or regionally-varying atmospheric circulation and turbulence. Effectively, each probe acts as a wind-borne tracer.

Although the science instruments would have ceased to function, the LEAVES probes would continue to descend ever more slowly, taking a total of 2100 minutes to reach the surface and covering a total ground track of nearly 3000 km. If we retain the original (30 km min altitude) configuration, the only modification is to replace the flexible Mylar panels with a material resistant to the 465° C surface, such as Zylon® (Toyobo Corporation).

Ongoing development at NASA Glenn Research Center is rapidly maturing SiC communications, sensors, memory, and processors (P. G. Neudeck, Spry, Chen, Prokop, & Krasowski, 2017; Spry et al., 2018) and it is expected that these components will eventually enable a new generation of Venus exploration at low altitudes and on the surface. It is likely, however, that this technology will continue to have higher power requirements than equivalent silicon electronics. A future generation of landed probes will be enabled by these developing technologies, but with a deliverable mass of tens of kilograms, the Long-Lived In-situ Solar System Explorer (LLISSE) (Kremic et al., 2017) represents a very different paradigm than LEAVES. We do not see a significant



advantage in growing the mass and power requirements to meet the expected performance of long-lived, robust, surface science platforms since such modifications would negate LEAVES' strengths of swarm-deployment, unshielded atmospheric entry, and low cost.

## 8 COST

The scope of cost estimates are based on conventional prime contractor costs only. We did not include NASA oversight, technology development, launch, Phase E (science analysis), education and public outreach, or integration with primary spacecraft. We assume a SEER-H guidance for a Class D mission, and flight hardware production of 100 units with 85% system level learning.

1: LEAVES
Σ 1.1: Electronics
1.1.1: Temp & Pressure Sensors
1.1.2: Mounting Plate
1.1.3: Data processing
1.1.4: Misc. Cabling
Σ 1.2: Comm Antenna
1.2.1: Hemi/Omni Antenna
Σ 1.3: Electrical Power Subsystem
1.3.1: Harness
1.3.2: Battery Li
1.3.3: Battery
Σ 1.4: Structures and Mechanisms
1.4.1: Main Bus

LEAVES Subsystem	Costs (FY18\$K)		
	DDT&E	FHW*	Total
Electronics	389.1	3,586	3,975
Comm Antenna	20.6	10	31
Electrical Power Subsystem	189.5	77	266
Structures and Mechanisms	87.4	289	376
PM/SE/SMA&AIT	435	455	890
<b>Subtotal</b>	<b>1,121</b>	<b>4,417</b>	<b>5,538</b>
Fee (10%)	112	442	554
<b>Total</b>	<b>1,233</b>	<b>4,858</b>	<b>6,092</b>

\*FHW includes 100 production units

### Approach: Bucketing all Electronics

Lump ADC, C&DH, and Comm together as a single electronics component.

Figure 31. Prime contract cost estimate

All costs in FY18\$K	Case 1 – v1
Development	\$1,200
Production (100 Units)	\$4,900
<b>Prime Contract Total</b>	<b>\$6,100</b>
Recurring for each unit (\$K)	~\$49K

Table 5. Total cost per LEAVES unit

## 9 PHASE I SUMMARY OF CONCLUSIONS

Our intensive design exercise, conducted with engineering and technical support of the Glenn Research Center's COMPASS group, validated the initial LEAVES concept. That is, that a high drag, slow descent probe could return valuable science

data on a planetary atmosphere. Our initial requirement, to eliminate the need for parachutes or balloons by having the structure act as a stabilized high-drag surface, was shown to be entirely viable. Moreover, because of the very low mass of each LEAVES probe and the relatively large surface area of the kite-like structure, our design has an additional and unexpected benefit... it requires no aeroshell in order to be deployed directly from orbit by a carrier spacecraft, dramatically reducing mass.

An operational lifetime of 9 hours in the target altitudes of 100 – 30 km puts means that LEAVES occupies a niche in exploration paradigms that is squarely between free-falling or parachuted probes (with descent times around 1 hour) and actively buoyant atmospheric platforms (with lifetimes of days to months) for a tiny fraction of the cost of these monolithic approaches.

Key to the viability and value of LEAVES is the swarm approach, which allows for a relatively large volume of science data to be obtained in a short amount of time. The redundancy provided by dozens or hundreds of economical probes results in a high fault tolerance and equally high mission resiliency.

By targeting specific science objectives that can be achieved with low power, low mass, low cost devices, LEAVES can contribute significantly to the state of knowledge of planetary atmospheres. For example, resolving the chemical and physical state of an atmosphere across a globally-extensive range of lateral and vertical locations at a specific point in time (or several) is beyond the capability of even a navigable long-lived aerial platform.

Active development of a new generation of high temperature electronics, sensors, and materials means that LEAVES could be viable to increased depth in the Venus atmosphere or even on the surface. This capability would translate directly the atmospheres of the gas giants, with the added benefit that wide bandgap electronics provide higher robustness in high radiation environments. Perhaps more compelling is the idea that LEAVES could serve as a platform for the detection of signs of life in planetary atmospheres. A wide geographic distribution of inexpensive probes, each carrying lightweight sensors that respond to specific molecular targets or evidence of metabolic activity, could effectively cast a wide net in the search for non-terrestrial life. In contrast to isolated searches on the surface of Mars, this would allow for the targeting of the whole of a specific potential biome (i.e. the habitable region of an atmosphere) and thereby provide a more robust confirmation of the presence or absence of biotics. In Earth's atmosphere this capability might be leveraged to study microorganisms and active chemical species throughout the atmospheric column. Although the suspended lifetime would be lower (due to lower density of the Earth's atmosphere relative to Venus), the value of low cost, swarm-type probes would be comparable.

We recognize that, by design, LEAVES must operate in tandem with the support of an orbiter that acts as a deployment platform, method of geolocation, and a relay of instrument data to Earth ground stations. Given the relatively short lifetime of LEAVES,

we anticipate that such a requirement would have only a marginal impact on an orbiting platform that would, in all likelihood, already be performing similar orbital maneuvers in order to take advantage of Venus' atmosphere for aerobraking and orbit circularizing. Directly deploying LEAVES during this process poses little risk for the primary spacecraft, but the narrow range of parameters that lead to a successful and safe capture of LEAVES to the Venus upper atmosphere suggests that more thorough analysis and modeling would need to be completed during future development. Likewise, the aerodynamic performance of a ballistically captured and free-falling inverted pyramid is modeled by analogy on that of a cone. We expect that robust fluid dynamics study would also be a key element in further development.

We began this study with a sound concept, based upon preliminary aerodynamic analyses, that represented a Technology Readiness Level (TRL) of 1-2. Our comprehensive study of the mission profile, structure, payload, and supporting requirements represent a successful maturation to TRL 2-3. Because all of the scientific payload is composed of components with TRL of 5-7 and the material behavior of structural elements is already well known, we project that LEAVES could be matured very rapidly with future study and development. Prototyping could be accomplished with low cost conventional components, with functional demonstrations in Earth's atmosphere through deployment from drone or high altitude balloon. Deployment from orbit (with some minor structural refinement) could demonstrate unprotected atmospheric entry and payload function during descent. Finally, a fully Venus-appropriate LEAVES, such as is described in this report, could be tested in a relevant chemical and physical environment in the Glenn Extreme Environment Rig (GEER) facility (Harvey et al., 2014) and at relevant orbital entry conditions through the use of wind tunnel testing. This means that LEAVES could be ready for proposal as a technology demonstration, secondary payload, or Stand Alone Mission of Opportunity (SALMON/SIMPLEX) within 3-5 years depending on support for further development and study.

## 10 REFERENCES

---

- Blamont, J. (1985). The exploration of the atmosphere of venus by balloons. *Advances in Space Research*, 5(9), 99–106. [https://doi.org/10.1016/0273-1177\(85\)90276-5](https://doi.org/10.1016/0273-1177(85)90276-5)
- Blamont, J. E., Sagdeev, R. Z., Linkin, V. M., Crisp, D., Elson, L. S., Golitsyn, G. S., ... Young, R. E. (1986). Implications of Preliminary VEGA Balloon Results for the Venus Atmosphere Dynamics. *Soviet Astronomy Letters*, 12, 22–25.
- Bluman, J. E., Kang, C.-K., Landrum, D. B., Fahimi, F., & Mesmer, B. (n.d.). Marsbee - Can a Bee Fly on Mars? In *55th AIAA Aerospace Sciences Meeting*. <https://doi.org/10.2514/6.2017-0328>
- Cutts, J. A., Nock, K. T., Jones, J. A., Rodriguez, G., & Balaram, J. (1995). Planetary exploration by robotic aerovehicles. *Autonomous Robots*, 2(4), 261–282. <https://doi.org/10.1007/BF00710794>
- DuPont. (2017). *DuPont Kapton Summary of Properties*. Retrieved from <http://www.dupont.com/content/dam/dupont/products-and-services/membranes-and->

films/polyimide-films/documents/DEC-Kapton-summary-of-properties.pdf

Esposito, L. W. (1984). Sulfur dioxide: episodic injection shows evidence for active venus volcanism. *Science (New York, N.Y.)*, 223(4640), 1072–1074. <https://doi.org/10.1126/science.223.4640.1072>

Forget, F., & Capderou, M. (2010). *A Simple Analytical Equation to Accurately Calculate the Atmospheric Drag During Aerobraking Campaigns*. Presented at the 8th International Planetary Probe Workshop.

Fukuhara, T., Futaguchi, M., Hashimoto, G. L., Horinouchi, T., Imamura, T., Iwagaimi, N., ... Yamazaki, A. (2017). Large stationary gravity wave in the atmosphere of Venus. *Nature Geoscience*, 10(2), 85–88. <https://doi.org/10.1038/ngeo2873>

Gel'man, B. G., Zolotukhin, V. G., Lamonov, N. I., Levchuk, B. V., Lipatov, A. N., Mukhin, L. M., ... Okhotnikov, B. P. (1979). Analysis of the chemical composition of the Venus atmosphere on the “Venera-12” automatic interplanetary station by means of a gas chromatograph. *Kosmicheskie Issledovaniya*, 17(5), 708–713.

Harvey, R., Radoman-Shaw, B., Jacobson, N. S., Vento, D., Costa, G., Kulis, M., ... Kremic, T. (2014). Venus in a Bottle: High Fidelity Simulation of Venus Surface Conditions with NASA's Glenn Extreme Environment Rig (GEER). *2014 GSA Annual Meeting in Vancouver, British Columbia*. Retrieved from [https://gsa.confex.com/gsa/2014AM/finalprogram/abstract\\_246498.htm](https://gsa.confex.com/gsa/2014AM/finalprogram/abstract_246498.htm)

Hensley, S., Smrekar, S. E., Mueller, N., Helbert, J., & Mazarico, E. (2016). VERITAS: Towards the Next Generation of Cartography for the Planet Venus. *ResearchGate*. Presented at the Lunar and Planetary Science Conference XLVII. Retrieved from [https://www.researchgate.net/publication/312312852\\_VERITAS\\_Towards\\_the\\_Next\\_Generation\\_of\\_Cartography\\_for\\_the\\_Planet\\_Venus](https://www.researchgate.net/publication/312312852_VERITAS_Towards_the_Next_Generation_of_Cartography_for_the_Planet_Venus)

Hoerner, S. F. (1965). *Fluid-dynamic drag: practical information on aerodynamic drag and hydrodynamic resistance*. Hoerner Fluid Dynamics.

Hunter, G. (2016, June 1). *High Temperature Rad-Hard Electronics, Atmospheric Measurements, and Sensor Systems for Venus Exploration and Other Planetary Missions*. Presented at the New Frontiers 4 Technology Workshop, Washington, DC.

Hunter, G. W., & Culley, D. (2012). Extreme Environment Electronics in NASA's Aeronautics Research. In *Extreme Environment Electronics* (pp. 41–48). Boca Raton, FL: CRC Press.

Khatuntsev, I. V., Patsaeva, M. V., Titov, D. V., Ignatiev, N. I., Turin, A. V., Limaye, S. S., ... Moissl, R. (2013). Cloud level winds from the Venus Express Monitoring Camera imaging. *Icarus*, 226(1), 140–158. <https://doi.org/10.1016/j.icarus.2013.05.018>

Kliore, A. J., Keating, G. M., & Moroz, V. I. (1992). Venus international reference atmosphere (1985). *Planetary and Space Science*, 40, 573–573. [https://doi.org/10.1016/0032-0633\(92\)90255-M](https://doi.org/10.1016/0032-0633(92)90255-M)

Kremic, T., Ponchak, G. E., Beheim, G. M., Okojie, R., Scardelletti, M. C., Wrbanek, J. D., ... Balcerski, J. (2017). *LONG-LIFE IN-SITU SOLAR SYSTEM EXPLORER (LLISSE) PROBE CONCEPT AND ENABLING. 2*.

Mahieux, A., Vandaele, A. C., Neefs, E., Robert, S., Wilquet, V., Drummond, R., ... Bertaux, J. L. (2010). Densities and temperatures in the Venus mesosphere and lower thermosphere retrieved from SOIR on board Venus Express: Retrieval technique. *Journal of Geophysical Research: Planets*, 115(E12). <https://doi.org/10.1029/2010JE003589>

Makel, D., & Carranza, S. (2015, April). *Development Of A Harsh Environment Gas Sensor Array For Venus Atmospheric Measurements*. Presented at the Venus Science Priorities for

Laboratory Measurements in Instrumentation Definition Workshop, Hampton, VA.

Marcq, E., Bertaux, J.-L., Montmessin, F., & Belyaev, D. (2013). Variations of sulphur dioxide at the cloud top of Venus's dynamic atmosphere. *Nature Geoscience*, 6(1), 25–28. <https://doi.org/10.1038/ngeo1650>

Neudeck, P. G., Spry, D. J., Chen, L., Prokop, N. F., & Krasowski, M. J. (2017). Demonstration of 4H-SiC Digital Integrated Circuits Above 800 °C. *IEEE Electron Device Letters*, 38(8), 1082–1085. <https://doi.org/10.1109/LED.2017.2719280>

Neudeck, Philip G., Meredith, R. D., Chen, L., Spry, D. J., Nakley, L. M., & Hunter, G. W. (2016). Prolonged silicon carbide integrated circuit operation in Venus surface atmospheric conditions. *AIP Advances*, 6(12), 125119. <https://doi.org/10.1063/1.4973429>

Oyama, V. I., Carle, G. C., Woeller, F., Pollack, J. B., Reynolds, R. T., & Craig, R. A. (1980). Pioneer Venus gas chromatography of the lower atmosphere of Venus. *Journal of Geophysical Research: Space Physics*, 85(A13), 7891–7902. <https://doi.org/10.1029/JA085iA13p07891>

Peralta, J., Lee, Y. J., Hueso, R., Clancy, R. T., Sandor, B. J., Sánchez-Lavega, A., ... Peach, D. (2017). Venus's winds and temperatures during the MESSENGER's flyby: An approximation to a three-dimensional instantaneous state of the atmosphere. *Geophysical Research Letters*, 44(8), 3907–3915. <https://doi.org/10.1002/2017GL072900>

Petersen, K., Andreyeva, K., Roggeveen, J., Cipolato, M., Adumitroaie, V., Quadrelli, M., ... Stoica, A. (2017). Windbots: An investigation of potential solutions for Jupiter-based aerostatic robotic explorers. *2017 IEEE Aerospace Conference*, 1–9. <https://doi.org/10.1109/AERO.2017.7943618>

Pollack, J. B., Ragent, B., Boese, R., Tomasko, M. G., Blamont, J., Knollenberg, R. G., ... Travis, L. (1979). Nature of the Ultraviolet Absorber in the Venus Clouds: Inferences Based on Pioneer Venus Data. *Science*, 205(4401), 76–79. <https://doi.org/10.1126/science.205.4401.76>

Short, K. B. (2014). *Printable Spacecraft: Flexible Electronic Platforms for NASA Missions. [Final Report: Early Stage Innovation, NASA Innovative Advanced Concepts (NIAC) Phase 2]*. Retrieved from <https://ntrs.nasa.gov/search.jsp?R=20190001174>

Spry, D. J., Neudeck, P. G., Lukco, D., Chen, L. Y., Krasowski, M. J., Prokop, N. F., ... Beheim, G. M. (2018). Prolonged 500°C Operation of 100+ Transistor Silicon Carbide Integrated Circuits. <https://doi.org/10.4028/www.scientific.net/MSF.924.949>

Titov, D. V., Bullock, M. A., Crisp, D., Renno, N. O., Taylor, F. W., & Zasova, L. V. (2013). Radiation in the Atmosphere of Venus. In *Exploring Venus as a Terrestrial Planet* (pp. 121–138). <https://doi.org/10.1029/176GM08>

Yamazaki, A., Yamada, M., Lee, Y. J., Watanabe, S., Horinouchi, T., Murakami, S., ... Nakamura, M. (2018). Ultraviolet imager on Venus orbiter Akatsuki and its initial results. *Earth, Planets and Space*, 70(1), 23. <https://doi.org/10.1186/s40623-017-0772-6>


Yavrouian, A., Plett, G., Yen, S., Cutts, J., & Baek, D. (1999). Evaluation of materials for Venus aerobot applications. In *Balloon Systems Conferences. International Balloon Technology Conference* (Vols. 1–0). <https://doi.org/10.2514/6.1999-3859>

Young, R. E. G. (2001, January 1). *Venus Multiprobe Mission*. Presented at the International Venus Workshop, Sagamihara, Japan. Retrieved from <https://ntrs.nasa.gov/search.jsp?R=20020038535>


Yung, Y. L., Liang, M. C., Jiang, X., Shia, R. L., Lee, C., Bézard, B., & Marcq, E. (2009). Evidence for carbonyl sulfide (OCS) conversion to CO in the lower atmosphere of Venus. *Journal of Geophysical Research E*, 114, E00B34.

# 11 APPENDIX

Included in the appendix below is an unannotated set of tables representing details of LEAVES master and subsystems. Further explanation of each subsystem is given in the preceding text.




## Systems Rollup




MEL Summary: Case 1 LEAVES CD-2018-156	Leaf
Main Subsystems	Basic Mass (kg)
Science	0.006
Attitude Determination and Control	0.001
Command & Data Handling	0.013
Communications and Tracking	0.016
Electrical Power Subsystem	0.017
Structures and Mechanisms	0.071
Element Total	0.124
Element Dry Mass (no prop,consum)	0.124
Element Mass Growth Allowance (Aggregate)	0.027
Additional System Level Growth (For 30% tot)	0.010
Total Wet Mass with 30% Growth	0.161

142



## Master Equipment List (MEL)



Description	Basic Mass	Growth	Growth	Total Mass
Case 1 LEAVES CD-2018-156	(kg)	(%)	(kg)	(kg)
LEAVES	0.1238	22.1%	0.0273	0.1511
Leaf	0.1238	22.1%	0.0273	0.1511
Science	0.0056	30.0%	0.0017	0.0073
Attitude Determination and Control	0.0012	10.0%	0.0001	0.0013
Command & Data Handling	0.0130	30.0%	0.0039	0.0169
Communications and Tracking	0.0155	10.0%	0.0016	0.0171
Electrical Power Subsystem	0.0173	41.9%	0.0073	0.0246
Structures and Mechanisms	0.0711	18.0%	0.0128	0.0840

143



# Powered Equipment List (PEL)



Description	Power Mode 1	Power Mode 2
Case 1 LEAVES CD-2018-156	Science Operation, No Comm	Communicating, No Science
	576 min	24 min
	(W)	(W)
<b>LEAVES</b>	<b>0.131</b>	<b>1.192</b>
<b>Leaf</b>	<b>0.131</b>	<b>1.192</b>
Science	0.045	0.000
Attitude Determination and Control	0.035	0.035
Command & Data Handling	0.050	0.050
Communications and Tracking	0.000	1.000
Electrical Power Subsystem	0.001	0.107
Structures and Mechanisms	0.000	0.000

144



## Case 1 - Leaf: Science



Description	QTY	Unit Mass	Basic Mass	Growth	Growth	Total Mass
Case 1 LEAVES CD-2018-156						
Science			0.0056	30.0%	0.0017	0.0073
Science Package Group One			0.0056	30.0%	0.0017	0.0073
Chemical Sensor Subassembly	1	0.0025	0.0025	30.0%	0.0008	0.0033
High Altitude Pressure Sensor	1	0.0006	0.0006	30.0%	0.0002	0.0008
MEMs Pressure Sensor	1	0.0005	0.0005	30.0%	0.0002	0.0007
Temperature Sensor	1	0.0005	0.0005	30.0%	0.0002	0.0007
Substrate	1	0.0010	0.0010	30.0%	0.0003	0.0013
FET and OP AMP	1	0.0005	0.0005	30.0%	0.0002	0.0007

145



## Case 1 - LEAT:

# Attitude Determination and Control



Description	QTY	Unit Mass	Basic Mass	Growth	Growth	Total Mass
Case 1 LEAVES CD-2018-156						
<b>Attitude Determination and Control</b>			<b>0.0012</b>	<b>10.0%</b>	<b>0.0001</b>	<b>0.0013</b>
<b>Guidance, Navigation, &amp; Control</b>			<b>0.0012</b>	<b>10.0%</b>	<b>0.0001</b>	<b>0.0013</b>
3-Axis Accelerometer	1	0.0012	0.0012	10.0%	0.0001	0.0013

146



## Case 1 - LEAT:

# Command and Data Handling



Description	QTY	Unit Mass	Basic Mass	Growth	Growth	Total Mass
Case 1 LEAVES CD-2018-156						
<b>Command &amp; Data Handling</b>			<b>0.0130</b>	<b>30.0%</b>	<b>0.0039</b>	<b>0.0169</b>
<b>C&amp;DH Hardware</b>			<b>0.0100</b>	<b>30.0%</b>	<b>0.0030</b>	<b>0.0130</b>
Microcontroller	1	0.0020	0.0020	30.0%	0.0006	0.0026
PCB	1	0.0020	0.0020	30.0%	0.0006	0.0026
1 MHZ Clock	1	0.0005	0.0005	30.0%	0.0002	0.0007
FET	1	0.0005	0.0005	30.0%	0.0002	0.0007
Inst. Op Amp	6	0.0005	0.0030	30.0%	0.0009	0.0039
Radar Detector	1	0.0010	0.0010	30.0%	0.0003	0.0013
Activation Pressure Switch	1	0.0010	0.0010	30.0%	0.0003	0.0013
<b>Instrumentation &amp; Wiring</b>			<b>0.0030</b>	<b>30.0%</b>	<b>0.0009</b>	<b>0.0039</b>
Misc. Cabling	1	0.0030	0.0030	30.0%	0.0009	0.0039

147





# Case 1 - Leat: Communications and Tracking



Description	QTY	Unit Mass	Basic Mass	Growth	Growth	Total Mass
Case 1 LEAVES CD-2018-156						
<b>Communications and Tracking</b>			<b>0.0155</b>	<b>10.0%</b>	<b>0.0016</b>	<b>0.0171</b>
<b>Ka Band System</b>			<b>0.0155</b>	<b>10.0%</b>	<b>0.0016</b>	<b>0.0171</b>
Vendor Ruggedized Micro Transmitter	1	0.0030	0.0030	10.0%	0.0003	0.0033
Vendor Hemi/Omni Antenna	1	0.0080	0.0080	10.0%	0.0008	0.0088
Specialized Cable	1	0.0045	0.0045	10.0%	0.0005	0.0050



# Case 1 - Leat: Electrical Power System



Description	QTY	Unit Mass	Basic Mass	Growth	Growth	Total Mass
Case 1 LEAVES CD-2018-156						
<b>Electrical Power Subsystem</b>			<b>0.0173</b>	<b>41.9%</b>	<b>0.0073</b>	<b>0.0246</b>
<b>Power Management &amp; Distribution</b>			<b>0.0053</b>	<b>46.2%</b>	<b>0.0025</b>	<b>0.0078</b>
Harness	1	0.0043	0.0043	50.0%	0.0022	0.0065
Voltage Regulator	1	0.0010	0.0010	30.0%	0.0003	0.0013
<b>Energy Storage</b>			<b>0.0120</b>	<b>40.0%</b>	<b>0.0048</b>	<b>0.0168</b>
Low Temperature Battery	2	0.0030	0.0060	30.0%	0.0018	0.0078
High Temperature Battery	2	0.0030	0.0060	50.0%	0.0030	0.0090



# Case 1 - LEAT: Structures and Mechanisms



Description	QTY	Unit Mass	Basic Mass	Growth	Growth	Total Mass
Case 1 LEAVES CD-2018-156						
<b>Structures and Mechanisms</b>			<b>0.0711</b>	<b>18.0%</b>	<b>0.0128</b>	<b>0.0840</b>
<b>Structures</b>			<b>0.0651</b>	<b>18.0%</b>	<b>0.0117</b>	<b>0.0769</b>
<i>Primary Structures</i>			0.0616	18.0%	0.0111	0.0727
Main Bus	1	0.0616	0.0616	18.0%	0.0111	0.0727
<i>Secondary Structures</i>			0.0036	18.0%	0.0006	0.0042
Instrument Mount	1	0.0036	0.0036	18.0%	0.0006	0.0042
<b>Mechanisms</b>			<b>0.0060</b>	<b>18.0%</b>	<b>0.0011</b>	<b>0.0071</b>
<i>Adaptors and Separation</i>			0.0060	18.0%	0.0011	0.0071
spring lock hinge	1	0.0060	0.0060	18.0%	0.0011	0.0071

## 12 ACKNOWLEDGEMENTS

---

We gratefully acknowledge the support of the NASA NIAC Program, under solicitation NNH17ZOA001N-18NIAC\_A1, for providing the resources for this study. We also thank the NASA Postdoctoral Program for partial support of PI Balcerski during initial proof-of-concept development.

This work was done the support of the Collaborative Modeling for Parametric Assessment of Space Systems (COMPASS) group at NASA's Glenn Research Center. Team members are identified below, with our thanks and appreciation.

Compass Lead - Steve Oleson

Compass Venus Expert – Geoff Landis

Lead System Integration, MEL, Science Payload - James Fittje

Mission, Mission Visualization, Launch vehicle – David Smith

AD&CS –Brent Faller, Mike Martini

Mechanical Systems - John Gyekenyesi

Thermal Descent - Tony Colozza

Power - Brandon Klefman

C&DH, Software- Nicholas Lantz

Communications and Tracking– Robert Jones

Configuration and Integration - Tom Packard

Cost – Jon Drexler